ADDIS ABABA UNIVERISTY

COLLEGE OF NATURAL SCIENCES

Automatic Sediment Detection in Urine Micrograph

Ameha Worku Gurmu

A Thesis Submitted to the Department of Computer Science in Partial Fulfillment for the Degree of Master of Science in Computer Science

Addis Ababa, Ethiopia

October 2018

ADDIS ABABA UNIVERISTY

COLLEGE OF NATURAL SCIENCES

Ameha Worku Gurmu

Advisor: Yaregal Assabie (PhD)

This is to certify that the thesis prepared by Ameha Worku, titled: *Detection of Sediments in Urine Micrograph* and submitted in partial fulfillment of the requirements for the Degree of Master of Science in Computer Science complies with the regulations of the University and meets the accepted standards with respect to originality and quality.

Signed by the Examining Committee:

	Name	Signature	Date
Advisor:	_____	_____	_____
Examiner:	_____	_____	_____
Examiner:	_____	_____	_____

ABSTRACT

Urine is one of the most complex fluid specimens found in our body. The concentration of urine sediments is an indication of various diseases. Invariably, medical facilities in our country employ manual approach to detect sediments under microscopes. However, medical results using manual approach are not always accurate. It could vary from person to person. Also, the approach is time consuming, and increases workloads of technicians. To mitigate these problems, scholars in the field recommend using automated detection of sediment in urine. However, ensuring accuracy from detection of se in urine remains challenging due to variations in urine color, irregular shape, and non-uniform illumination. Hence, in this research a better segmentation and feature extraction technique is proposed to detect urine sediments.

Urine microscopic input image is improved by grayscale image, adaptive median filtering, and image adjustment which in turn yield uniform illumination for further analysis task. This study proposes a fusion of adaptive threshold, canny edge detection and morphological operations to isolate the background from the foreground and remove tiny objects. In this regard, a total of twenty-three features are extracted from shape, texture and color of urine to represent white blood cells, red blood cells, epithelia cells, and crystal in urine microscopic image. Finally, classification models are built using Neural Network and Multi Class Support Vector Machine. The performance of each model is compared using tenfold cross validation technique. Compared to other methods, this technique demonstrated acceptable detection performance with average sensitivity of 95.34%, specificity of 98.10%, precision of 90.22%, and accuracy of 95.93% using neural network classifier and an average sensitivity of 90.38%, specificity of 98.01%, precision of 91.68%, and accuracy of 97.40% using multiclass support vector machine for white blood cell(WBC), red blood cell(RBC), epithelial cell(EP) and Crystal, respectively. The performance of the proposed prototype is found to be effective for the identification of sediment in urine sample even in the context where sediment in urine have irregular shape, different color and poorly illuminated microscopic images.

Keywords: Multiclass Support Vector Machine, Neural Network, Urine Micrograph

ACKNOWLEDGEMENTS

First and foremost, I thank the Almighty God for the strength and good health HE bestowed upon me to accomplish my research endeavor.

Next, I am indebted to my advisor, Dr. Yaregal Assabie, for his constant support, guidance and encouragement since the inception of the thesis to its completion. I have immensely benefitted from his insights over the course of the research period. I must appreciate his patience in commenting draft chapters of the thesis and the wisdom of his supervision in general when I started to think for myself and become relatively independent. I also thank my postgraduate instructor Dr. Mulugeta Libsie and the whole computer science department staff for many valuable discussions during the past three years. Indeed, this thesis would not have the shape and substance it has today without the intellectual inputs of the above scholars. My sincere thanks also goes to the staff of Tikur Anbessa Hospital / Urine and Pathology Department/, who dedicated their time for providing support and supplying equipment.

I would like to thank my lovely daughter Sipara Ameha for giving me more time to focus on my research thereby enduring the pain of my absence. Indeed, her endless love was the source of my happiness and energy.

I would like to thank my mother Yesamashew Wolde-Micheal, my sisters Hirut Worku and Dr. Muluembet Worku for their relentless support. I may not be able to stand where I am now without their constant encouragement. You have a special place in my heart.

Finally, I would like to thank my friends for their continuous motivation and encouragement during my stay in the university.

TABLE OF CONTENTS

LIST OF FIGURES

LIST OF TABLES

LIST OF ALGORITHMS

ACRONYMS AND ABBREVIATIONS

AOS	Additive Operator splitting
AMF	Adaptive Media Filtering
DIP	Digital Image Processing
EP	Epithelial Cell
GIP	Digital Image Processing
GLCM	Gray Level Co-occurrence Matrix
HPF	High Power Field
LDA	Linear Discriminant Analysis.
LoG	Laplacian of Gaussian
MBR	Minimum Bounding Rectangle
MBS	Microscopic Blood Sample
MBSI	Microscopic Blood Sample Image
MUSI	Microscopic Urine Sample Image
NN	Neural Networks
PDA	Personal Digital Assistant
RBC	Red Blood Cell
ROI	Region of Interest
SEP	Squamous Epithelial Cell
SVM	Support Vector Machine
UTI	Urinary Track Infection
WBC	White Blood Cell
YC	Yeast Cell

CHAPTER ONE: INTRODUCTION

1.1 Background

Medical, architectural, advertising, design and fashion companies capture and store numerous digital images. As a result, large image databases are being created and used in many applications. The focus of this study is on medical images which hospitals and medical institutions generate and store in digital formats stemming from their day-to-day activities.

One such medical image is microscopic urine image. Urine is the most complex body fluid specimen. Potentially, urine contains meaningful types of elements. Kidneys are the responsible organs in the renal system. Renal system in humans includes kidneys, where urine is produced, and the ureters, bladder, and urethra for the passage, storage, and voiding of urine. Kidneys help to regulate the amount of water in the body, filter blood before sending it back to the heart, conserve proteins, electrolytes, and other compounds. Anything that is not needed by the body is discharged through urine which travels from the kidneys through the urethra, and out of the body [1].

Urine consists primarily of water between 91% to 96% with organic solutes and sediments. It is generally yellow and relatively clear. Every time someone urinates, the color, quantity, concentration, and content of the urine will be slightly different because of its varied constituent elements. The presence and concentration of urine sediments deviating from the normal is an indication of various diseases such as urine track infection, renal diseases, bladder defects and other illnesses [2].

The presence and concentration of sediments, often composed of microscopic particles, various kinds of cells, cast and mucus, are clinically tested by taking urine which is one of the most easily accessible biological samples [3]. It might be examined using manual urinalysis, semi-automated urinalysis, or automated microscopic urine sediment examination. Among these clinical tests manual microscopic urine sediment examination is used mostly in clinical laboratories to identify cells like white blood cells (WBCs), red blood cells (RBCs), epithelial cells (EPs), yeast cell, crystal and cast [1].

In manual urine microscopy examinations, laboratory technicians observe sediments in microscopic image under the microscope and judge the kinds and amounts of sediments that exist in urine sample. Usually, the results are estimated. The outcome of such examination depends on the skill, experience, and motivation of the technician who carried out the task [4]. In addition to these problems, manual microscopic urine sediment examination is labor-intensive, time-consuming, imprecise, and inaccurate [5].

With the development of science and technology, some scientists have conducted researches on detection and segmentation of microscopic image in urine sample with the aim of overcoming the limitations of manual examination. The researches focused on various themes including the detection of red blood cell in urine micrograph, it focuses on detection of RBCs in urine image which is captured under microscope using image processing techniques [7]. Automatic method for classification and recognition of sediments, mainly white and red blood cells in urinary sediment, have been also carried out using image processing techniques such as media filtering for image pretreatment, select and extract features as feature vectors for classification and recognition, and finally developed support vector machine(SVM) classifier to distinguish sediments in the image [8], automated recognition of urinary epithelial cell, it focuses only on detection of epithelial cell which is one of the particle in urine, using image processing techniques such as segmentation, textural features extraction and classification to get the result [9]. But, sediment in urine are not very clear, the image itself has an ambiguous and the illumination is not uniform. In addition, sediments are located in different depth, and different cells have varied reflection property even when they have the same depth.

In this research, the presence of cells such as red, white and epithelial and crystal sediment in poorly illuminated microscopic urine image which affect human health conditions will be detected using image processing technique.

The renal system in humans regulates the amount of water in the body, filters blood before sending it back to the heart and conserves essential compounds. Anything that is not needed by the body is excreted in the form of urine such as white blood cell, red blood cell, cast, crystal and other particle or sediment. Figure 1.1[10] shows sediments in urine sample.

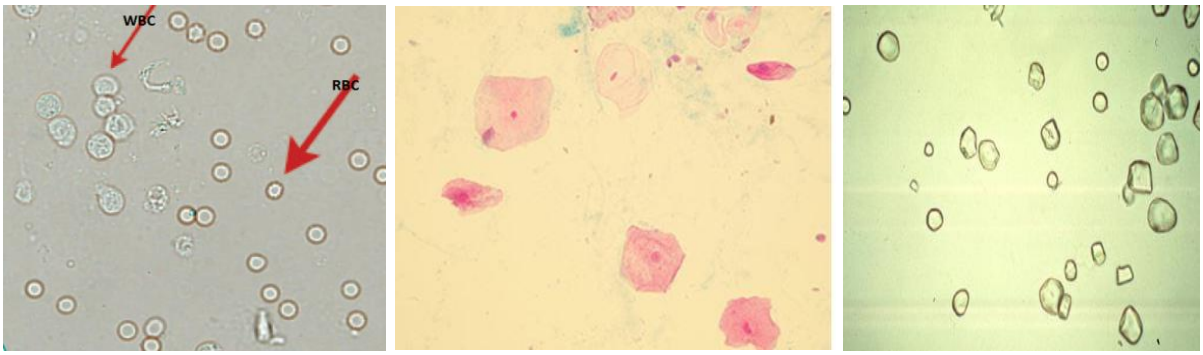

(A) (B) (C)

Figure 1.1: Image of (A)Red Blood cell and white blood cell, (B) Epithelial, (C) Crystal in Different Illumination

1.2 Motivation

Urine may be a waste product, but it contains not only enormous but also useful information about the state of human conditions, i.e., physical and physiological [9]. In addition to the simplicity of its acquisition, it is one of the most commonly analyzed specimens during medical examinations [4]. Urine analysis in Ethiopia is usually conducted using traditional detection method, notably manually operated microscope observation. This involves taking a drop of concentrated urine sediment from specimen and diagnosing sediments in microscopic and then judge the kinds and the level of sediment concentration in the urine. Among other issues, the results from such examination depend on the skill, experience and motivation of the technician mandated for the task. As a consequence, results are subjective, less reliable and thus, inconclusive. In addition, traditional method of urine analysis is characterized by low efficiency and difficult getting conclusion because of heavy workload of technician. This motivated us to implement automatic urine sediment detection system that accurately detects and classifies particles in urine sample.

1.3 Statement of the Problem

Due to the development of computer technology and image processing algorithms, many researchers have attempted to overcome the limitations of manual microscopic blood examination using image processing techniques, specially to examine blood sample [11, 12, 13, 14]. Despite remarkable achievements, results from researches on blood samples cannot be directly applied to examine urine because the edge of urine sediment is not very clear, color differences between

blood and urine and sediments in urine possess irregular shape. Also, urine illumination is not uniform.

Thus, researches have been conducted separately on detection of sediments in urine sample using image processing techniques [7, 11, 12]. However, those researches are not accurately detecting and classifying sediments in urine due to poorly illuminated microscopic image and irregular shape of sediment in urine. Furthermore, only some components of the sediments are detected and classified separately. Therefore, the purpose of this study is to accurately detect and classify the occurrence of sediments in urine microscopic image using better image processing approaches.

1.4 Objectives

General Objective

The general objective of this research is to develop automatic detection algorithm that detects and classifies sediments in urine sample using image processing techniques.

Specific Objectives

The study has the following specific objectives:

- Review related literature for better understanding of the techniques and methods.
- Collect microscopic urine image to detect and classify sediments in urine.
- Design a segmentation algorithm for detecting sediments in microscopic urine image
- Extract feature vectors from segmented sediments for classifying particle in urine image.
- Develop a prototype for automatically detecting and classifying sediments in urine microscopic image.
- Test and evaluate the performance of the system using sample data.

1.5 Research Methods

The research methods used to conduct the study includes the following:

- **Literature Review**

  To understand the subject matter, literatures related to the work will be reviewed. This helps to summarize all related works that are relevant to this work.

- **Data Collection**

  Sample data will be collected from database and image capture from microscope.

- **Feature Extraction**

  Geometric, statistical texture and color features will be extracted to model sediments in urine microscopic image.

- **Prototype development**

  MATLAB version R2017a will be used to implement the prototype of the system and Visio 2013 will be used for designing the system architecture and algorithms.

- **Experimental Evaluations**

  To evaluate the system in scientific way, sample data that will be collected from different sources will be fed into the developed prototype. Then, the system will be evaluated by comparing its output against the manually observed data.

1.6 Scope and Limitations

Microscopic urine analysis is examined for red blood cells, white blood cells, epithelial cells, casts, bacteria, yeast, and crystals. Among these particles, red blood cells, white blood cells, epithelial cells and crystal are extremely important and routine analyses to state the health condition of a person. Because of rare existence of cast and yeast in urine, they are not considered in this work.

1.7 Application of Results

The outcomes of this research will benefit patients, specialists and the health sector in general. Some of the advantages are:

- It provides reliable, faster and convenient detection method of sediments in urine micrograph for medical purpose.
- It reduces the time that patients will have to spend in medical centers to get results since the system will timely examine the presence of sediment in urine.
- It reduces workloads, long time microscope observation and visibility problems of lab technicians thereby saving him/her from issuing false positive results.

- It might also reduce the likelihood of damages to lab technicians vision rate due to microscope's refraction behavior.
- Detection and classification of sediments in urine micrograph will be done automatically.

1.8 Organization of the Rest of the Thesis

The remaining part of the thesis is organized as follows. Chapter Two reviews existing literature on automatic sediment detection. Chapter Three reviews related works. The design of automatic sediment detection is presented in Chapter Four. The evaluation, test results and discussions are presented in Chapter Five. Finally, Chapter Six presents the conclusions of the study and eventually identifies potential areas for future research.

CHAPTER TWO: LITERATURE REVIEW

2.1 Introduction

In this Chapter, the basic concepts regarding sediment in urine and its diagnosis process related to this thesis are discussed. It begins with a brief urine introduction and its morphological structure through which urine constituent and normal concentration of segments in urine are discussed. The distinction between manual versus automated sediment detection in urine are also discussed. The general approaches for automatic detection of sediment in urine are presented. In addition, digital image processing techniques, such as image segmentation, feature extraction and classification, which are useful tools across several applications, are presented.

Hence, this Chapter is organized in Three sections: Urine sediment and its morphological structure, urine diagnosis and digital image processing (DIP) approaches to urine sediment and finally ends by summary.

2.2 Urine Sediments and its Morphological Structure

Urine is one of the most complex body fluid specimens. It potentially contains a number of meaningful types of elements to state the health condition of human being [1]. Due to this, health care institutes, examine urine to know the type of diseases. The main sediment examined in urine includes red blood cells, white blood cells, epithelial cells, casts, bacteria, yeast, and crystals and their morphological structure is important for extracting features and classification of sediments.

Red blood cell

RBCs are the most important and largest amount of cell in human blood. The main function of RBC is to carry oxygen and delivering to the cells in the body [15]. RBCs exist in the urine because of bleeding at any point in the urogenital system from the glomerulus to the ureter [1]. A few, less than 2 RBCs per high-power field, are present in the urine of a healthy person [16]. The number of RBCs exceeding this number is an indication of the presence of different diseases.

The morphological structure of RBCs in urine is mostly normal biconcave and 7-8 microns. RBC in urine is shown as concentric circles and this concentric circle is basically the center of the cell [7]. The size of RBCs is smaller than WBC but sometimes and rarely the two could have the same size. The RBC has a clear edge and it resembles a circle plate. But, the morphological structure of

RBCs in microscopic examination could vary. They may appear normally shaped, swollen by dilute urine (in fact, only cell ghosts and free hemoglobin may remain), or cremated by concentrated urine. Figure 2.1 [10] shows various RBC morphological structure in urine.

Figure 2.1: Morphological Structure of RBC in Urine

White blood cell

In addition to RBCs, blood also contains WBCs Like RBC, WBC occurs in urine due to bleeding at any point in the urogenital system. The normal number of WBCs that exist in urine is 2-5 WBCs per hpf microscope. The presence of more number of WBCs in urine than the normal amount is an indication of infection, inflammation, or contamination.

The morphological structure of WBC is spherical in shape, 10–12 microns with large nucleus, granular cytoplasm and mostly lager than RBC. Based on their morphological appearance, WBCs are clustered into five types of cells. These are neutrophils, eosinophil, basophils, lymphocyte, and monocyte. All of these WBC types are found in plasma, but the predominant type found in plasma and urine is neutrophil [17]. The size, nucleus, and cytoplasmic structure of white blood cells are some of the properties that distinguish it from RBC. Sometimes WBC also contains granular cytoplasm, although not always easy to identify it. Usually, WBCs are found joined with each other and sometimes with sediment constituents [8]. Generally, WBC has vague edge and its gray scale distribution does not balance. So, shape and texture features are distinguishing elements of WBC [8]. Accordingly, the morphological structure of WBCs in microscopic examination could vary. Figure 2.2 [10] shows the morphological structure of white blood cells in urine.

Figure 2.2: Morphological Structure of White blood Cells in Urine

Squamous Epithelial Cell

The most common type of cell seen in the urine sediment is the squamous epithelial cell. A squamous epithelial cell is a large flattened cell with abundant cytoplasm and small round central nucleus. Although squamous epithelial cells have little clinical significance, they must be differentiated from other cellular elements. Scientists agree that the urine of a healthy person contain less or equal to 15-20 squamous epithelial cells per hpf microscope [18]. Figure 2.3 [10] shows the morphological structure of squamous epithelial cell.

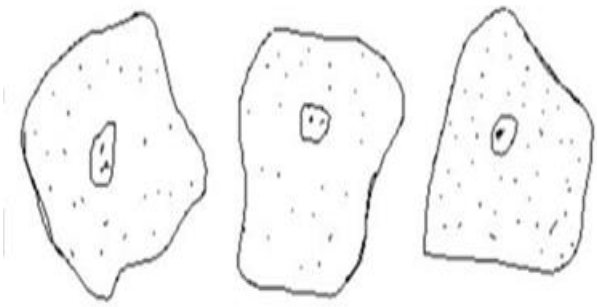

Figure 2.3: Morphological structure of Squamous Epithelial in Urine

Crystal

Urine contains different chemicals. Sometimes these chemicals form solids particles called crystals. Laboratory technician look at the amount, size and the type in urine examination. Larger crystals or specific types of crystals can become kidney stones. Kidney stones are hard, pebble-

like substances stuck in the kidneys. A stone can be as small as a grain of sand, as big as a pea, or even larger [18]. Figure 2.4 [10] shows the morphological structure of crystal in urine sample.

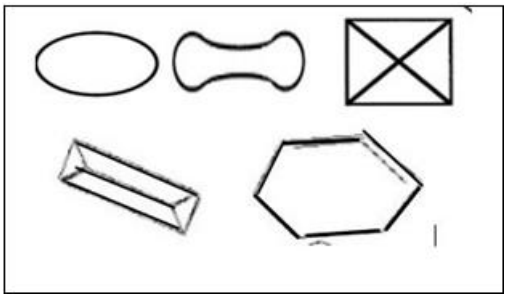

Figure 2.4: Morphological Structure of Crystal in Urine

2.3 Urine Diagnosis

Each day, health organizations commonly recommend to drink eight glasses of water, which equals about 2 liters, or half a gallon. The intake water and their substances needed by the organisms are largely absorbed and the remaining “worthless” substance is extracted. The intake water is extracted from the body in different forms. Urine is one of the different forms and the largest amount of liquid extracted from the body. It is the most complex body fluid specimens: it potentially contains about 60 meaningful types of elements such as water and dissolved low-molecular blood constituents [1].

The presence and concentration of urine sediments deviating from the normal is an indication of various diseases. The examination or counting the quantity of different visible components in urinary sediment can be done in manual or semi-automated ways. Traditional method performed by a laboratory technician using a microscope is known as urinalysis and the other one is semi-automated method [3].

2.3.1 Urinalysis

Urinalysis is one of the most famous medical tests used to measure or describe elements of urine. It has a very important role in diagnosis of urologic conditions such as calculi, urinary tract infection (UTI) and malignancy, and indicate the presence of systemic diseases affecting the kidneys. It also has an indispensable role to the identification of casts, RBC, WBC EP, crystals, yeast, and cast.

Microscopic examination involves taking a drop of concentrated urine sediment from a spun aliquot of the specimen, well-mixed urine (usually 10-15 ml) which is centrifuged in a test tube at relatively low speed (about 2-3,000 rpm) for 5-10 minutes. The supinate is decanted and a volume of 0.2 to 0.5 ml will be left inside the tube. Then a drop of suspended sediment is poured onto a glass slide and cover slipped by a glass cover [18]. Figure 2.5 [18] shows specimen parts.

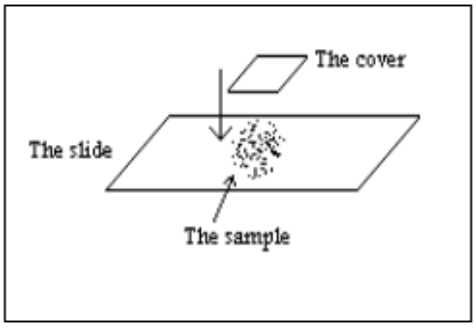

Figure 2.5: Specimen Parts

In urinalysis, the laboratory technician observes sediments in microscopic image through the microscope and judge, the kinds and amounts of sediments. The method of concentrating the urine specimen can be variable depending on the procedure used and the technique of the technologist [19].

A urinalysis does not give accurate results because they examine large number of samples. The examination procedure is also burdensome to lab technicians that they sometimes make mistakes [6]. These problems require fast and efficient methods for detection of sediment in urine sample to prevent false diagnosis. Figure 2.6 [10, 20] shows the list of sediments' images that appear inside urine specimen under microscope.

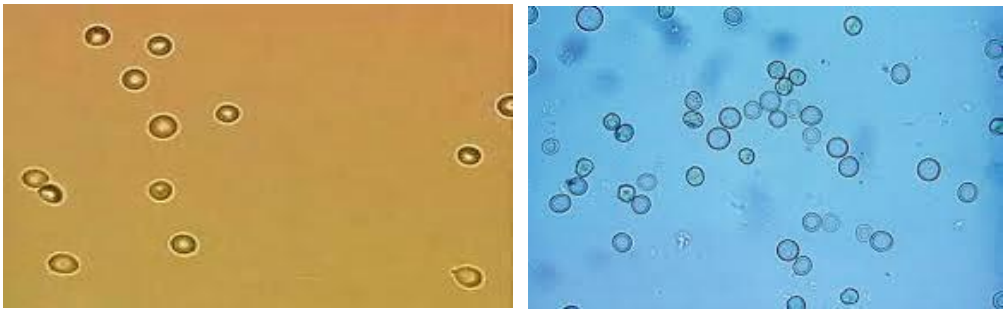

(a)

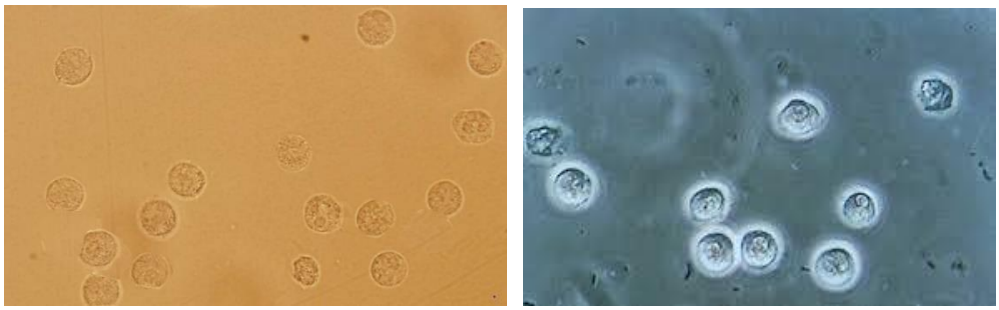

(b)

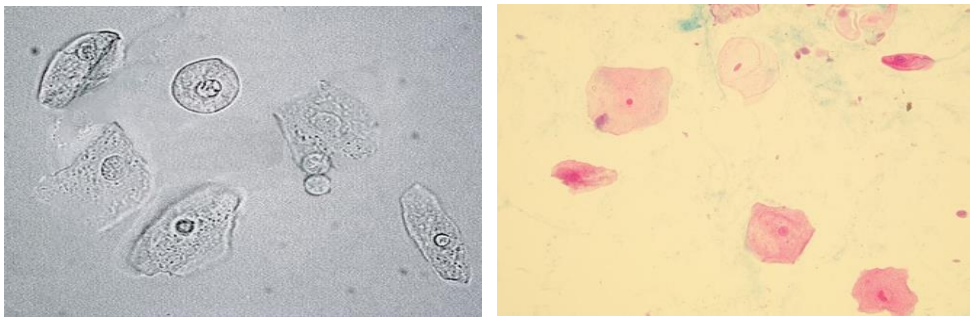

(c)

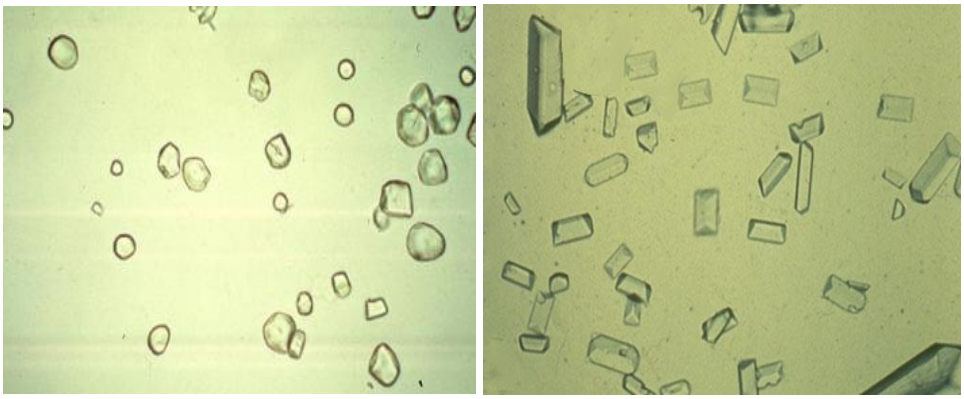

(d)

Figure 2.6: Urine Sediments; (a) RBC, (b) WBC, (c) EP, (d)Crystal in Different Microscopic Adjustment

2.3.2 Automatic Sediment Detection

The study of detecting and recognition in microscopic images is becoming practical important field of study from time to time and commendable results have been achieved [21, 22]. The

detection and recognition of microscopic urine sediment is one of these fields attracting the attention of academics and practitioners.

2.4 Approaches to Automatic Sediment Detection in Urine

An image may be defined as a two-dimensional function, *f* (x, y), where x and y are spatial (plane) coordinates, and the amplitude *f* at any pair of coordinates (x, y) is called the intensity or gray level of the image at that point. When x, y, and the intensity values of *f* are all finite, discrete quantities, we call the image a digital image. A digital image is composed of a finite number of elements, each of which has a location and value. These elements are called picture elements, image elements, pels, or pixels. Pixel is the term used most widely to denote the elements of a digital image [23].

Generally, any microscopic image detection system has five main processes: image acquisition, pre-processing, segmentation, feature extraction and classification.

2.4.1 Input Data and Image Acquisition

The first step in digital image processing is image acquisition, i.e., to acquire a digital image. A urine sample is collected in an unused disposable plastic cup with a tight-fitting lid. A randomly voided sample is suitable for routine urinalyses as well as image acquisition. A drop of suspended sediment is poured onto a glass slide and cover slipped by a glass cover. Then acquiring image will be carried out using microscopic camera or camera-mounted microscope designed for this purpose in different controlled environments.

One of the challenges in taking microscopy image is the introduction of photometric variant [24] such as shadow/shading, and highlights. Consequently, the occurrence of inconvenient color temperature (illumination) under different environments results in less quality image [25]

2.4.2 Image Preprocessing

Image pre-processing is the term for operations on images at the lowest level of abstraction. These operations do not increase image information content, but they decrease if entropy is an information measure [26, 27]. The aim of pre-processing is improvement of the image data that suppresses undesired distortions or enhances some image features relevant for further processing and analysis task [28].

As noted above, in image acquisition the original urine microscopic image often degrades by noise such as shadow/shading, highlights, and inconvenient color temperature. It is necessary to preprocess the image to get accurate information about the edge [29]. In this regard, a set of sequential processes such as creating gray scale image, enhancing image, and removing small or unnecessary objects to improve the original urine microscopic image after image acquired is necessary [28].

a) Creating Gray Scale Image

A color image contains more useful information but also contains a lot of redundant information [3]. Color image transformed to grey image reduces the memory spending, restrains the noise and thus does not clearly identify urinary sediment. This creates an image with high contrast and clear contour which is useful to post-processing [23].

The following image conversion formula is to change color image to gray image:

$$f(x, y) = R(x, y) \times 0.3 + G(x, y) \times 0.59 + B(x, y) \times 0.11 \quad (1)$$

where $f(x, y)$ is the gray value of pixel point (x, y) in gray image, $R(x, y)$, $G(x, y)$, and $B(x, y)$ are respectively R, G, B tri-color weight at point (x, y) in color image.

b) Median Filtering

Unwanted noise can result from dust sediments that could be present on the slide. It is necessary to filter the image so as to eliminate the noise. Median filtering is more effective in image smoothening and preserves edges while removing noise. Median filtering techniques have been applied using this formula [23].

$$V(m, n) = median\{y(m - k, n-1), (k, 1) \in W\} \quad (2)$$

where W is a suitably chosen window, m is the number of columns and n the number of rows in the chosen window. The algorithm for median filtering requires arranging the pixel values in the window in increasing or decreasing order and picking the middle value. If Nw is even, then the median is taken as the average of the two values in the middle. If Nw is odd the median is taken as middle value which specifies the window size.

This technique calculates the median of the surrounding pixels to determine the new demonized value of the pixel. A median is calculated by sorting all pixel values by their size, then selecting

the median value as the new value for the pixel. The amount of pixels which should be used to calculate the median. For each pixel, a 3 x 3, 5 x 5, 7 x 7, 9 x 9, 11 x 11 window of neighborhood pixels are extracted, and the pixel intensity values are arranged in ascending order and the median value is calculated for that window. The intensity value of the center pixel is replaced with the median value. This procedure is done for all the pixels in the image to smoothen the edges of Magnetic Resonance Image. High Resolution Image was obtained when using 3 x 3 than 5 x 5 and so on. Figure 2.7 Shows the median filtering.

4	0	3	1	0	5
2	2	4	1	4	3
1	0	1	0	2	0
2	5	4	1	2	5
1	1	4	2	3	0
1	3	0	2	5	0

4	0	3	1	0	5
2	2	1	1	1	3
1	2	1	2	2	0
2	1	1	2	2	5
1	1	4	2	2	0
1	3	0	2	5	0

Figure 2.7: Values Before and After Applying Midian Filtering

2.4.3 Image Segmentation

Image segmentation is the division of an image into regions or categories to correspond to different objects or its parts. Every pixel in an image is allocated to one of these categories. The level to which the subdivision is carried depends on the problem being solved. That is, segmentation should stop when the objects of interest have been isolated. In the automated inspection of electronic assemblies, interest lies in analyzing images of the products with the objective of determining the presence or absence of anomalies, such as missing components or broken connection paths. There is no reason to carry segmentation past the level of detail required to identify those elements [23].

Segmentation involves complex procedures and requires more processing time compared with other methods. Otherwise, it is the most important step because the feature extraction and counting

depends on the correct segmentation of sediments. If segmentation is well-done, then all other stages in image analysis would become easy to handle or execute.

Generally, segmentation algorithms for monochrome images are based on one of the two basic properties of image intensity values: discontinuity and similarity. In the first case, the approach involves partitioning an image based on abrupt changes in intensity, such as point, line and edges. Sobel, Robert, Prewitt, Laplacian, and Canny operators fall in this category. The principal task in the second category is partitioning an image into regions that are similar according to a set of predefined criteria. Thresholding and region base methods belong to this category [23].

a) Edge Detection

Although point and line detection certainly are important in any discussion on image segmentation, edge detection is by far the most common approach for detecting meaningful discontinuities in intensity values. Such discontinuities are detected by using first- and second-order derivatives.

The edge detection operation is essentially an operation carried out to detect significant local changes in intensity level of an image. The tool of choice for finding edge strength and direction at location *(x, y)* is the gradient of the image. In other words, the first-order derivative of choice in image processing is the gradient. Since an image *f (x, y)* is a two-dimensional function its gradient is a vector [23, 30].

The gradient of a 2-D function, f(x, y), is defined as the vector. The magnitude of this vector can be calculated using equation 3.

$$\nabla f = \begin{bmatrix} g_x \\ g_y \end{bmatrix} = \begin{bmatrix} \frac{\partial f}{\partial x} \\ \frac{\partial f}{\partial y} \end{bmatrix} \tag{3}$$

The magnitude of this vector

$$mag(\nabla \boldsymbol{f}) = \left[g_x^2 + g_y^2\right]^{½} \tag{4}$$

$$= \left[\left(\frac{\partial y}{\partial x}\right)^2 + \left(\frac{\partial y}{\partial x}\right)^2\right]^{½}$$

Often, this quantity is approximated by absolute values:(5)

$$\nabla f \approx |g_x| + |g_y| \tag{6}$$

These approximations still behave as derivatives; that is, they are zero in areas of constant intensity and their values are related to the degree of intensity change in areas of variable intensity. It is a common practice to refer to the magnitude of the gradient or its approximations simply as "the gradient." A fundamental property of the gradient vector is that it points in the direction of the maximum rate of change of f at coordinates (x, y). The angle at which this maximum rate of change can be calculated using equation 7.

$$\alpha(x, y) = tan^{-1}\left(\frac{g_y}{g_x}\right) \quad (7)$$

Second-order derivatives in image processing generally are computed using the Laplacian of a 2-D function *f(x, y) which* formed from second-order derivatives and it can be calculated using equation 8.

$$\nabla^2 f(x, y) = \frac{\partial^2 f(x,y)}{\partial x} + \frac{\partial^2 f(x,y)}{\partial y} \quad (8)$$

The Laplacian seldom is used directly for edge detection because, as a second order derivative, it is unacceptably sensitive to noise, its magnitude produces double edges, and it is unable to detect edge direction. However, the Laplacian can be a powerful complement when used in combination with other edge-detection techniques [48].

The basic idea behind edge detection is to find places in an image where the intensity changes rapidly, using one of the following general criteria:

1. Find places where the first derivative of the intensity is greater in magnitude than a specified threshold.
2. Find places where the second derivative of the intensity has a zero crossing.

Function edge in Image processing toolbox provides several edge estimators based on the criteria just discussed. For some of these estimators, it is possible to specify whether the edge detector is sensitive to either horizontal or vertical edges or both. The general syntax for this function is shown in equation 7.

$$[g, t] = edge(f, 'method', parameters) \quad (9)$$

where f is the input image, method is among Sobel, Prewitt, Roberts, Laplacian of Gaussian (LoG) and Canny. The parameters are additional restrictions. In the output, g is a logical array with 1s at the locations where edge points were detected in f and 0s elsewhere. Parameter t is optional; it gives the threshold used by edge to determine which gradient values are strong enough to be called edge points.

b) Threshold

Image thresholding classifies pixels into two categories. The first category contains those at which some property measured from the image falls below a threshold in one category, those at which the property equals or exceeds a threshold belong to the second category.

Suppose an image, *f (x, y),* composed of light objects with dark background where the object and background pixels have intensity levels grouped into two dominant modes. One way of extracting the objects from the background is to select a threshold *T* that separates these modes. Then any image point *(x, y)* at which *f (x, y) > T* is called an object (or foreground) point. Otherwise, the point is called a background point (the reverse holds true for dark objects on a light background). The threshold (binary) image *g (x, y)* can be presented using equation 10.

$$g(x,y) = \begin{cases} a, & if f(x,y) > T \\ b, & if\ f(x,y) \leq T \end{cases} \quad (10)$$

Pixels labeled "a" correspond to objects where as pixels labeled "b" correspond to the background. Usually and by convention, $a = 1$ (white) and $b = 0$ (black). Threshold method can be viewed in two different approaches known global or adaptive thresholding and variable threshold:

Global Thresholding: When T is a constant applicable over an entire image, the preceding equation 10 is referred to as global thresholding. There are two ways of choosing threshold in global thresholding. One way to choose a threshold (T) is by visual inspection of the image histogram which is easy to choose a threshold T that separates them. Another way to choose *T* is by trial and error which involves selecting different thresholds till identifying the one that produces good result, as judged by the observer. This is particularly effective in an interactive environment.

Variable Threshold: If the value of *T* changes over an image, then it is variable thresholding. The term local or regional thresholding is also used to denote variable thresholding in which the value of T at any point (x, y) in an image depends on properties of a neighborhood of (x, y). In this regard, the average intensity of the pixels in the neighborhood is one good example. If T depends on the spatial coordinates (x, y) themselves, then variable thresholding is often referred to as dynamic or adaptive thresholding. The standard deviation and mean of pixels in a neighborhood of every point in an image is the basic approach for local Threshold. These two quantities are quite useful for determining local thresholds because they are descriptors of local contrast and average intensity.

Equation for local threshold

Let σ and m denote the standard deviation and mean value of the set of pixels contained in a neighborhood centered at coordinates (x, y) in an image [23, 30]. Then common form of variable thresholds is:

$$T_{xy} = \sigma_{xy}\,\mathrm{a} + b\sigma_{xy} \tag{11}$$

Where a and b nonnegative constant, and other useful form is

$$T_{xy} = \sigma_{xy}\,\mathrm{a} + b\mathrm{m_G} \tag{12}$$

where $\mathrm{m_G}$ is mean of the global image. The segmented image is computed as:

$$g(x,y) = \begin{cases} a, & iff(x,y) > T_{xy} \\ b, & if\ f(x,y) \le T_{xy} \end{cases} \tag{13}$$

Where f (x, y) is an input image, it evaluates for all pixel location in the image, and a different threshold is computed at each location (x, y) using the pixel in the neighborhood.

c) Watershed Segmentation

Segmentation by watershed embodies many concepts and often produces more stable segmentation results including connected segmentation boundaries. The approach also provides a simple framework to incorporate knowledge-based constraint in the segmentation.

Watershed segmentation Equation

Let g(s,t) be set denoting the coordinates of the points in the regional minima of an image . Let C(s,t) be a set denoting thecoordiates of the points in the catchment basin associated with reginal minimum . The notation min and max will be used to denote the minimum and the maximum values. Finaly, let T[n] represent the set of coordinates (s, t) for which g(s, t) < n, that is,

$$T[n] = \{(s, t) \mid g(s, t) < n\} \quad (14)$$

Geometrically, T[n] is the set of coordinate points in g(x, y) lying below the plane g(x, y)=n. The topography will be flooded in integer flood incrementes, from n = min + 1 to n = max + 1. At any step n of the flooding process, the algorthem needs to know the number of point below the flood depth. The coordinate in T[n] that is below the plane g(x, y) = n are "marked " blank, and all other coordinates are marked white.

- **Microscopic urine image Segmentation**

In automatic detection system, accurate segmentation process needs to be performed because feature extraction and counting depends on segmentation process.

2.4.4 Feature Extraction

After an image has been segmented into regions by methods of segmentation, the next step is to represent and describe the aggregate of segmented "raw" pixels in a form suitable for further computer processing. Feature extraction is one of the most important fields in image processing. It is used to extract the most relevant features of an image thereby assigning a label. In image classification, the crucial step is to analyze the properties of image features and to organize the numerical features into classes. In other words, an image is classified according to its contents [31].

The performance of the classification model and the accuracy rate of the classification itself largely depend on the numerical properties of various image features which represent the classification model's data. The major objective of feature extraction is to extract a set of features, which maximizes the recognition rate with the least number of elements and to generate similar feature set for varied instances of the same symbol.

Representing or describing a region involves two basic choices. The first has to do with representing the region in terms of its internal characteristics, i.e., boundary and the second relates with representing the region in terms of its internal characteristics, i.e., the pixels comprising the

region. An external representation is chosen when the primary focus is on shape characteristics. An internal representation is selected when the focus in on regional properties, such as color and texture. In general, feature extraction techniques are classified as color, shape, and texture [23, 25, 31].

a) Color Feature

In image analysis various color spaces are used to distinguish between images. These color spaces include RGB, CMY, HSV and others. An RGB (Red, Green, and Blue) color image is an M X N X 3 array of color pixels where each color pixel is a triplet corresponding to the red, green, and blue components of an RGB image at specific spatial location. HSV (Hue, Saturation, Value) is one of the several color systems used by people to select colors (e.g., of paints or inks) from a color wheel or palette. The HSV color space is formulated by looking at the RGB color cube along palette. CMY (Cyan, Magenta, and Yellow) are the secondary colors of light or, alternatively, the primary colors of pigments [23, 29].

There are two major advantages of using color vision. First, color provides extra information which allows to identify various physical causes for color variations in the world, such as changes due to shadows, light source reflections, and object reflectance variations. Second, color is an important tool to distinguish property of objects [25].

Color coherence vectors, color moments based and color correlogram are used for extraction features in an image. These techniques are based on extracting the mean, skewness, and standard deviation of intensity of the image pixel. Out of these methods color moment is the simplest, compact and robust technique to extract features [31].

b) Shape Feature

Shape features are used in in-object recognition and shape description. Shape feature extraction method can be classified into two groups. These are contour based and region-based methods. Whereas contour-based technique calculates shape feature from boundaries of an image only, region-based method extracts feature from the entire region. Contour based methods involve two approaches. The first is a continuous approach which does not divide shape into subparts. It uses the integral boundary to derive the feature vector. The second, discrete (Global) approach, divides the shape boundary into sub-parts and computes the multi-dimensional feature vector. The shape

descriptor involves calculating area, circularity, eccentricity, major axis orientation, and bending energy. In region-based techniques, all the pixels within a shape region are taken into account to obtain the shape representation, rather than only use boundary information as in contour-based methods. Common region-based methods use moment descriptors to describe shapes. Other region-based methods include grid method, shape matrix, convex hull and media axis [23 ,31].

c) Texture Feature

Texture is an important property of image. Such property of an image is a powerful regional descriptor and helps in the retrieval process. It measures the properties of an image such as smoothens, coarseness and regularity. The three principal approaches used in image processing to describe the texture of the region are statistical, structural, and spectral. Statistical approaches yield characterization of textures as smooth, coarse and grainy. Structural techniques deal with the arrangement of image primitives, such as the description of texture based on regularly spaced parallel lines. Spectral techniques are based on properties of the Fourier spectrum and are used primarily to detect global periodicity in an image by identifying high energy, narrow peaks in the spectrum [23]. Gabor filter or wavelets is widely used to extract texture features for image classification. Gabor filter or wavelets characterize an image by obtaining the center frequency and orientation parameter.

2.4.5 Classification

Object recognition is an important task in image processing and computer vision. It is concerned with determining the identity of an object being observed in an image from a set of known tags or features. Humans can recognize any object in the real world easily without any efforts; on the contrary machines by itself cannot recognize objects. Thus, the basic thing in object recognition is to design a classifier, which takes a set of known tags of objects as its input and indicates to which class the object belongs.

The intent of the classification process in an image processing is to categorize all pixels in a digital image into one of several classes, or “themes”. Classification algorithms consist two phases of processing which is training and testing. In the initial training phase, characteristic properties of typical image features are isolated and, based on these, a unique description of each classification category, i.e., training class, is created. In the subsequent testing phase, these feature-space

partitions are used to classify image features. There are several techniques that used for classification. Some of them are decision Tree, K-Nearest Neighbor, Support Vector Machines, and Neural Network [32].

Neural Networks: Neural Network use gradient descent method based on biological nervous system having multiple interrelated processing elements. These elements are known as neurons.

Rules are extracted from the trained neural network to improve interoperability of the learned network. To solve a problem, NN uses neurons which are organized processing elements. An NN changes its structure and adjusts its weight in order to minimize the error. Adjustment of weight is based on the information that flows internally and externally through the network during the learning phase. In NN multiclass, problem may be addressed by using multilayer feed forward technique in which neurons have been employed in the output layer rather using one neuron [32].

K-Nearest neighbor: This classifier is based on learning by training samples. Each sample represents a point in an n-dimensional space. All training samples are stored in an n-dimensional pattern space. When given an unknown sample, a k-nearest neighbor classifier searches the pattern space for the k training samples that are closest to the unknown sample. "Closeness" is defined in terms of Euclidean distance, where the Euclidean distance between two points, $X=(x_1, x_2, x_3,,……, y_n)$ and $Y=(y_1, y_2, y_3,…., y_n)$ is denoted by d(X, Y).

Nearest neighbor classifiers assign equal weight to each attribute. Nearest neighbor classifiers can also be used for prediction, that is, to return a real-valued prediction for a given unknown sample.

Support Vector Machine: SVM is a very effective method for regression, classification, and general pattern recognition. It is considered a good classifier because of its high generalization performance without the need to add a priori knowledge, even when the dimension of the input space is very high. For a linearly separable dataset, a linear classification function corresponds to a separating hyper plane f(x) that passes through the middle of the two classes, separating the two. SVMs were initially developed for binary classification but it could be efficiently extended for multiclass problems.

2.5 Model Evaluation Techniques

Model Evaluation is an integral part of the model development process. It helps to find the best model that represents our data and how well the chosen model will work in the future. Evaluating

model performance with the data used for training is not acceptable because it can easily generate over optimistic and over fitted models. There are two methods of evaluating models, Hold-Out and Cross-Validation. To avoid overfitting, both methods use a test set (not seen by the model) to evaluate model performance [33].

Hold-Out: In this method, the mostly large dataset is randomly divided in to three subsets

- **Test set** or unseen example is a subset of the dataset to assess the likely future performance of a model. If a model fits to the training set much better than it fits the test set, overfitting is probably the cause.
- **Training set** is a subset of the dataset used to build predictive models.
- **Validation set** is a subset of the dataset used to assess the performance of the model built in the training phase. It provides a test platform for fine tuning model's parameters and selecting the best-performing model. Not all modeling algorithms need a validation set.

K-fold Cross-Validation: When only a limited amount of data is available to achieve an unbiased estimate of the model performance, we use k-fold cross-validation. In k-fold cross-validation, the initial data are randomly partitioned into k mutually exclusive subsets or "folds," D1, D2, . . ., Dk, each of approximately equal size. Training and testing are performed k times. In iteration i partition Di is reserved as the test set, and the remaining partitions are collectively used to train the model. That is, in the first iteration, subsets *D*2, … *Dk* collectively serve as the training set to obtain a first model, which is tested on *D*1; the second iteration is trained on subsets *D*1, *D*3, … *Dk* and tested on *D*2; and so on. Unlike the holdout methods above, here, each sample is used the same number of times for training and once for testing. For classification, the accuracy estimate is the overall number of correct classifications from the *k* iterations, divided by the total number of tuples in the initial data [32].

Confusion Matrix

A confusion matrix is a table that is often used to describe the performance of a classification model (or "classifier") on a set of test data for which the true values are known. It allows the visualization of the performance of an algorithm. Given m classes, a confusion matrix is a table of at least size m by m. An entry, confusion matrix j, j in the first m rows and m columns indicates the number of tuples of class i that were labeled by the classifier as class j. For a classifier to have

good accuracy, ideally most of the tuples would be represented along the diagonal of the confusion matrix, from entry confusion matrix 1, 1 to entry Confusion Matrix m, m, with the rest of the entries being close to zero. The table may have additional rows or columns to provide totals or recognition rates per class [32, 34].

Receiver Operating Characteristic

ROC curves are a useful visual tool for comparing two classification models. ROC curves are two dimensional graphs that visually depict the performance and performance trade off a classification model. To construct ROC curve, two performance metrics are to be used. They are true positive rate (TPR) and false positive rate (FPR). ROC graphs are constructed by plotting the true positive rate against the false positive rate.

An ROC curve for M is plotted by starting at the bottom left-hand corner (where the true positive rate and false-positive rate are both 0), we check the actual class label of the tuple at the top of the list. If we have a true positive (that is, a positive tuple that was correctly classified), then on the ROC curve, we move up and plot a point. If, instead, the tuple really belongs to the "no" class, we have a false positive. On the ROC curve, we move right and plot a point. This process is repeated for each of the test tuples, each time moving up on the curve for a true positive or toward the right for a false positive [33, 34].

2.6 Summary

In this Chapter, general background regarding sediment in urine and its diagnosis process have been discussed. The distinction between urinalysis (manual) and automatic RBC, WBC, EP and crystal detection are presented. Approach to automatic sediment detection is also presented. In addition, the morphological structure of RBC, WBC, EPs and Crystal are presented. Digital image processing such as preprocessing, segmentation, feature extraction, classification and model evaluation technique, which are the major processes in automatic sediment detection in urine are also discussed.

In digital image, a set of sequential preprocessing to improve the original microscopic image after image is acquired, segmentation algorithms for representing a region in terms of its internal and external characteristics of an image and model evaluation technique to find the best model that

classify the data are discussed in detail. However, those general image processing algorithms do not specifically detect and classify sediments in urine sample.

CHAPTER THREE: RELATED WORK

3.1 Introduction

In recent years, with the development of computer technology and image processing algorithms, several corporations have been developing automatic urinary sediment analyzer [11, 12,14, 10]. In this Chapter, previous works related to detection, segmentation, and estimation of cells in urine and blood samples are reviewed. The research works related to detection of cells using digital image processing could be categorized into two groups based on the area of research. The first group is detection of cells in urine sample and the second group is detection of cells in blood sample. Gaps that exist in previous works related to detection, segmentation, and estimation of cells in blood and urine samples are also identified.

3.2 Detection of Cells in Blood Sample

Mohmood and Mansor [35] performed a research on RBC estimation using Hough transform technique. Their research work was to produce a computer vision system that can detect and estimate the number of RBC in the blood sample. RBC counting was done using three techniques which are logical, morphology and Hough transform. These algorithms used the shape of RBC for counting process. To reduce the noise and at the same time to enhance the image, two common image processing techniques were used. These are analyses in Hue Saturation Value (HSV) color space and the green component image. To estimate the number of red blood cells in the blood they used morphological erosion and median techniques. The tested data consists only 10 samples and produced the accurate estimation rate closest to 96% from manual counting.

Pavithra and Bagyamani [36] performed a research on WBC analysis using watershed and circular hough transform technique. This paper presents complete and fully automatic method for WBC analysis from Microscopic Blood Sample Image (MBSI). The whole work is developed using MATLAB environment. To identify and discover blood cells from each other, the research proposed two methods. First, RGB image is converted to gray level image and some image processing operations such as edge detection using sobel operator, image smoothing using median filtering, unsharp masking, and watershed are applied. Lastly, morphological operations and circular Hough transform are used for the final count. The proposed method was tested on 20 images of European Leukemia image and were found to be efficient in terms of cost consuming

compared to existing techniques of blood cell analysis. This method provides more accurate result for segmentation but more complex and require more processing time in comparison with other methods.

Shirvoikar and Virani [37] performed a research on detection and segmentation of WBC cells using Image processing techniques. This research provides user friendly software based on MATLAB allowing for quick user interaction with a simple tool for the detection and segmentation of WBC from images of blood samples. In order to perform the segmentation, it uses the techniques such as green plane extraction, arithmetic operations, linear contrast stretching, histogram equalization and global thresholding. They use minimum filter to improve the segmentation result and superimposing resulted nucleus on the original image helps in result verification. This algorithm has been applied to five types of WBC with successful isolation of WBC nucleus part from other blood components in an image. Total number of images tested is 594 and the experimental result shows the accuracy for the proposed algorithm for WBC cell segmentation to be 95.73%.

3.3 Detection of Sediment in Urine Sample

Ranzato *et al.* [12] proposed a general-purpose system to recognize biological sediments in urine images. This research is composed of four stages. First, promising locations in the image are detected and small regions containing interesting samples are extracted using a feature finder. Second, differential invariants of the brightness are computed at multiple scales of resolution. Third, after point-wise nonlinear mappings to a higher dimensional feature space, this information is averaged over the whole region thus producing a vector of features for each sample that is invariant with respect to rotation and translation. Finally, each sample is classified using a classifier obtained from a mixture-of-Gaussians generative model. This system was developed to classify 12 categories of sediments found in human urine. In all these applications, detection and classification are difficult because strong variability of objects of interest and because the background can be very noisy and highly variable. Their accuracy in cell recognition is unsatisfied in practical application because of the high significance of sediments in medical diagnosis.

Lou *et al.* [5] performed research on segmentation of urinary sediment based on Mumford-Shah algorithm. This paper proposed a mathematical model based on Mumford-Shah and then developed the corresponding Euler-Lagrange equation by Gateaux derivative method. The model

overcomes the active contour method by different active contour models and gave the numerical discrete scheme by Additive Operator Splitting (AOS). In order to optimize the computational efficiency of this processing step, they used additive operator splitting scheme on the nonlinear diffusion equation at each time step. The accuracy of AOS scheme is suitable for processing active contour segmentation but it requires long time, several iterative steps and only focuses as on the structure of the object.

Cao *et al.* [7] studied of red blood cells in urine image captured under microscope by image processing. This paper focuses on the detection of RBC in urine image captured under microscope by image processing techniques. They assumed that the original urine microscopic image is often degraded by noise and the sampling distribution of the Gaussian assumption in general is not supported in the case of small samples. This research work proposed improved Soble operator to provide more accurate information about the edge and round detection method by Hough transform is used to separate the red cell from the background. Based on Hough transform, the authors used the geometrical feature to detect the circle center in the image. They stated that the proposed method was relatively reliable and convenient detective method of the RBC in urine micrograph. Still, the structure information obtained is discontinuous and incomplete.

Li *et al.* [13] proposed an approach for casts detection and recognition. It consists of three steps, in the detection step, they used 4-direction variance map followed by an adaptive threshold method to transform the original image to binary image and then segment the cell paths from the whole image. By using this method, they obtained a good result in the segmentation step. They said experimental results is satisfactory in segmentation, achieves an easy-implemented, time-saving classifier and has improved recognition performance. However, in the recognition step, they extracted four shape features and one texture feature to send to a decision-tree classifier to do the classification. As they used area saturation, which is the ratio of object area to the area of its Minimum Bounding Rectangle (MBR) to describe the shape feature, while this is helpless as for the curved casts. They just used transparent degree to describe the texture feature which can easily make false identification with respect to some mucus and cell clumps which also have the tube-like shape.

Yang *et al.* [11] proposed a method for casts recognition in urinary microscopic sediment. They did a combination of shape and texture characteristics of casts in two steps. In the first step, a

modified method expresses the casts' tube-like shape feature stems from the traditional one which is based on the MBR. Instead of using MBR, they made use of the centerline to describe its shape while curved casts are concerned. Then, in the next step, some texture features are extracted and sent to the SVM classifier for further judgment. As this method is quite focused on the features of casts, both shape and texture, they said it is very effective to recognize casts in urinary sediment images. They tested on large amounts of urinary sediment microscopic images. Their dataset was collected of urinary sediment images in several hospitals. They achieved high accuracy in casts recognition. However, there exists some flat rejection phenomenon because of bad imaging system or pathological changes. To overcome these problems, more powerful and effective texture features should be considered.

Zhou and Zhout [8] proposed an automatic method for classification and recognition of sediments mainly WBC and RBC in urinary sediment. It is composed of three stages: First, original urinary sediment microscopic images are transformed into binary image by image pretreatment including median filtering, color image conversion to gray scale image and image segmentation. Second, they select and extract some features as feature vectors for classification and recognition. lastly, eleven texture and shape characteristics of casts are extracted from both gray scale image and binary image. Based on these characteristics, they developed an SVM classifier to distinguish casts from other sediments in the image. They said performance is better than traditional methods and it also offers the subject quantify measure, excellent diagnostic project and the doctor classify standardization. However, the existence of uneven illumination problem which is not considered in their experiment.

Almadhoun [9] performed a research on automated recognition of urinary EP. This paper introduces a comprehensive approach for automating procedures for detecting and recognition of EP in microscopic urine images. In this research images are segmented, textural features are extracted, features selection is applied, and finally five classifiers are tested to get the best results. Repeated experiments are done for adjusting factors to produce the best evaluation results. A very good performance was achieved compared with many related works. But they only considered Epithelial cell of the urine which is one of the components of urine sediment

3.4 Automatic Microscopic Urine Detection

The study of detecting and recognition in microscopic images is becoming practical important field of study from time to time and commendable results have been achieved [21, 22]. The detection and recognition of microscopic urine sediment is one of these fields attracting the attention of academics and practitioners. One notable achievement in this regard is that of the IRIS Company of America. The Company invented the IQ200 automated urine analyzer to diagnose urine sediments. But its effect is not as good as it predicts [5]. Later, Ranzato *et al*. [12] proposed a general-purpose system to recognize biological sediments in urine images. Similarly, Shen and Rui. [26] came up with harry wavelet feature which is used to extract each component of sediments. Their model used multi-class SVM classifier to classify each class. The results from the above two methods are commendable but not satisfactory because both of them followed similar approaches for every class of cell. Thus, the practicality of the models is rather limited. In Li *et al*. [4] formulated a novel method to resolve the problem of automatically detecting sediments' location in images. Liu *et al*. [24] proposed another method which uses computer image recognition and SVM technology. The method is useful to process automatically sampling image and analyze and diagnose diseases. Yang *et al*. [11] also used an efficient cast recognition algorithm in urinary sediments image. Notwithstanding, the contribution of these findings to the field of study, notably to automatic detection and classification of sediments in urinary sediment, performance in cells recognition are unsatisfactory [6]. Urine sediments in microscopic image are very small, possess irregular shape, and the image itself is fuzzy. Also, the illumination is not uniform, and the edge of urine sediment is not very clear. The inadequacy of results from the above methods in detecting and recognition urine microscopic images suggests the need for further research in the field.

3.4.1 Microscopic Urine Image Segmentation

In automatic detection system, accurate segmentation process needs to be performed because feature extraction and counting depends on segmentation process. There have been some literature concerning segment urine image in the early years. One notable work in this regard is *Li et al*. [38]. Li *et al.* used Gabor-based combining with texture segmentation method to segment the sediments from background image. Meanwhile, Li [4] used Gabor-based combining iterative method to segment the sediments from the image. The Gabor wavelet representation captures salient visual

properties such as spatial localization, orientation selectivity, and spatial frequency characteristic. Later, Luo *et al*. [5] introduced a mathematical model based on Mumford-Shah then they developed the corresponding Euler-Lagrange equation by Gateaux derivative method. Cao *et al.* [7] proposed a method to detect red cells in urine micrograph by used improved Sobel operator. Zhou and Zhou [8] adopted adaptive bi-threshold segmentation algorithm. Li *et al.* [39] applied an improved adaptive bi-threshold segmentation algorithm to the 4-direction variance mapping image. The method produced satisfactory segmentation.

In urine, microscopic image shows uneven illumination problem, i.e., different cells have varied reflecting property even with the same depth. It is also common that sediments in the same image render different contrast against background. Image threshold segmentation is a suitable approach for poorly illuminated image like microscopic image. Furthermore, it encompasses comprehensive information, which is crucial for the remaining tasks in the analysis process.

3.4.2 Feature Extraction for Microscopic Urine Image

The widely used feature extraction methods in detection and recognition of cells in urine are feature extraction technique based on morphology. Shen and Lue [26] extracted harr wavelet feature of each component. Liu *et al.* [24] proposed features extracted and selected by principal Component analysis (PCA). Luo *et al.* [40] extract features by considering invariant moments, granulometric measurements and domain specific features. They apply a feature selection procedure that reduces the number of features and happens to keep almost all the domain specific features.

Under different conditions, the performance of different feature detectors will be significantly different. The nature of the background, existence of other objects (occlusion), and illumination must be considered to determine the kind of features that can be efficiently and reliably detected.

In addition, to capture the necessary feature of an image more feature vectors or the combinations of feature are necessary in classifying an object.

3.4.3 Classification techniques for Microscopic Urine Image

Several classifiers have been done to recognize cells and sediment in urine sample. Luo *et al.* [40] classify with an SVM to obtain an overall average accuracy. Liu and Sun [24] adopt SVM learning algorithm to classify urinary sediment visible components. Uebele *et al.* [41] use a neural-network-

based fuzzy classifier on a dataset of blood cells. Ronneberger *et al.* [42] use a support vector machine (SVM) to classify them. Murasaki *et al.* [28] proposed multi-class SVM classifier to classify each class, recognized the substances using the fuzzy-neural networks in which the features membership functions are also obtained from the binarized images, Zeng *et al.* [43] categorized sediments of interests by neural networks and fuzzy reasoning. Dong *et al.* [44] developed a naïve Bayesian classifier after distinguishing the visible compositions. A sufficient classifier with high efficiency is needed to distinguish RBCs, WBCs, EP and Crystal in urine because recognition stage needs efficient classifier. Therefore, for this research work we have used a combination of NN and SVM classifier because of its high generalization performance without the need to add a priori knowledge, even when the dimension of the input space is very high.

3.5 Summary

This Chapter presented previous works related to detection, segmentation, and estimation of cells in blood and sediment in urine microscopic image. Some of the research works done on detection and counting of RBC and WBC in blood samples reported accurate results. However, the techniques used in blood microscopic image cannot be directly applied to urine microscopic image because the edges of RBC and WBC in urine have their own color, they possess irregular shape, and their illumination are not uniform and clear.

As a result, some researches were carried out on detection of RBC and EP in urine microscopic image. But, those researches in urine show strong variability of objects due to noise and the structure information obtained is discontinuous and incomplete. Besides these, the existence of uneven illumination problem and other sediment presented in the urine which is important to indicate the health condition of human being are not considered. Accordingly, a unified model that detects and classifies the respective class of sediment in urine in a given sample is needed.

CHAPTER FOUR: DESIGN OF AUTOMATIC URINE SEDIMINTS DETECTION SYSTEM

4.1 Introduction

As discussed previously, the study of detecting and recognition of microscopic images is becoming of practical importance. It is very convenient and time-saving to detect and classify an object in a microscopic image. However, almost all of the existing analyzers' performance in detection and recognition of sediment on microscopic urine image is unsatisfactory. In this thesis, therefore, automatic sediment detection and classification system in microscopic urine image that enables better performance is proposed. Therefore, in the Chapter the system architecture and its detail techniques for the proposed solution are described in detail.

4.2 System Architecture

The overall digital image processes technique for detection and classification of an object from microscopic urine image is almost similar. However, a set of different sequential techniques in creating gray scale image, enhancing image, removing small or unnecessary objects, or segmenting an object provide better accuracy and performance result. In addition, the combination of color, shape, and texture feature extraction methods keep much information from segmented object and this makes our system a better classifier. Hence, those techniques incorporated in the proposed system architecture are different from the other previous attempted works.

The system architecture consists of four major components namely, preprocessing, segmentation, feature extraction and sediment classification. First, Sample date are taken from Masaryk University database which is used for research purpose and image are also taken from a camera-mounted in microscope under different control environments. Then set of sequential processes such as smoothing, creating gray scale image, enhancing and segmenting image are applied. Features that are best suited to represent the sediments in the image are extracted from the image using an image analysis technique. Based on the extracted features multiple support vector (MSVM) and neural network (NN) machine learning techniques are applied to create model. Finally, 10-fold cross validation and confusion matrix were applied to examine the performance

of the system. Figure 4.1 shows the proposed system architecture for automatic sediment detection of microscopic urine image.

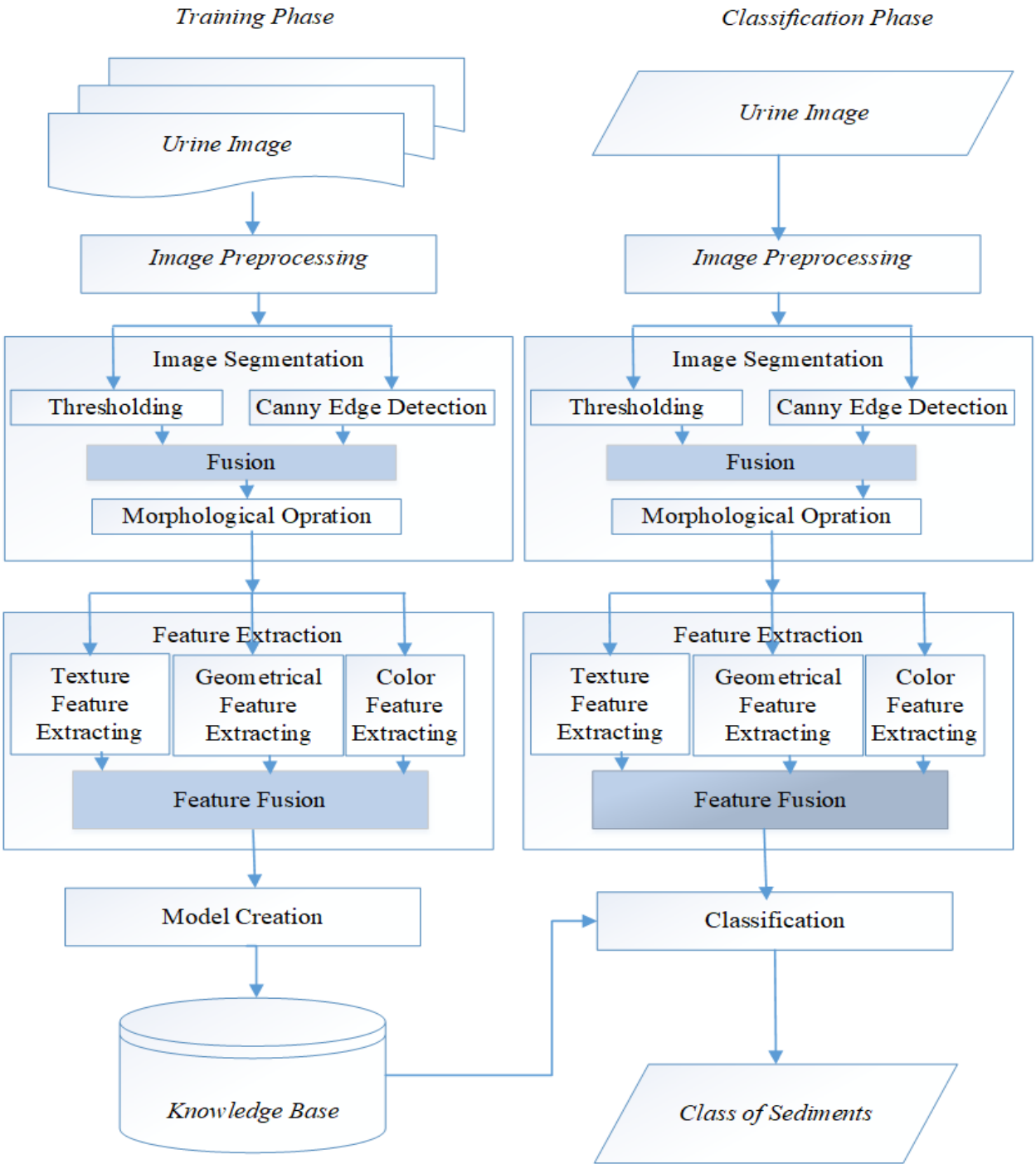

Figure 4.1: The General Architecture of Automatic Sediment Detection

4.3 Image Acquisition

Sample date are taken from Masaryk University database which is used for research purpose. In addition, image is capture using a camera-mounted in microscope under different control environment. In both case, camera-mounted in microscope, computer and another related device are responsible for acquiring the image. Figure 4.2 shows urine microscopic image.

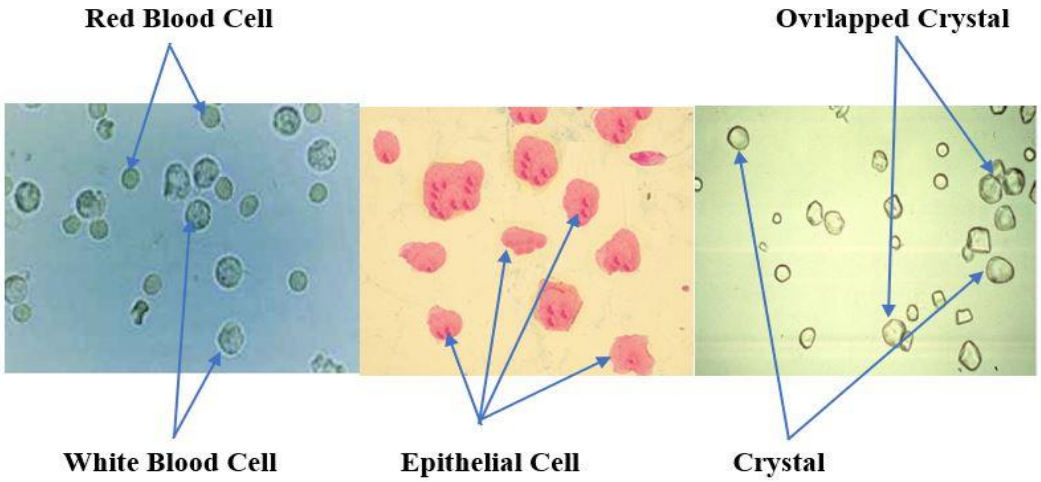

A B C

Figure 4.2: Urine Specimen Observation by Applying Different Microscopic Adjustment

4.4 Preprocessing

The aim of pre-processing in the proposed architecture is to improve the quality of microscopic urine image by suppressing unnecessary parts of the image which is important for the subsequent image processing task. The pre-processing has three components: Grayscale image, smoothing and image adjustment.

4.4.1 GrayScale Image

This sub component is responsible for transforming microscopic urine image into greyscale image. Image acquired from the suspended urine sample using camera-mounted in microscope is color or RGB image. This RGB image color information doesn't help us to identify important edges since one urine sample can produced is different color intensity due to applying different microscopic

adjustment. In addition, it is possible to only modern computers to perform simple pixel-by-pixel processing of a megapixel image in milliseconds. This is due to the intensity of each color channel is usually stored in eight bits, which indicates that the quantization level is 256. That is, a pixel in a color image requires a total storage of 24 bits. A 24-bit memory can be expressed as 2^{24}=16777216. On the contrary, there are 256 gray levels in an 8-bit gray scale image and the intensity of each pixel can have from 0 to 255, with 0 being black and 255 being white.

Hence, we converted microscopic color image into greyscale image and get clear image which is useful for the post-processing phases. Simultaneously it restrains the noise in the color image, easy to operate and reduces the memory required by the image. Figure 4.3 shows grayscale microscopic image urine. Algorithm 4.1 shows color image to grayscale conversion algorithm.

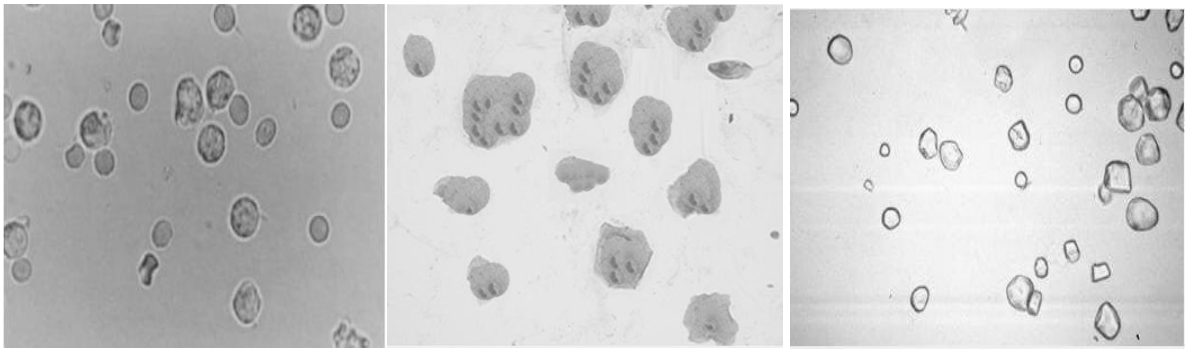

(A) (B) (C)

Figure 4.3: Grayscale microscopic urine image for (A) White and Red Blood Cells, (B) Epithelial cell and (C) Crystal

Input: A sample microscopic **urine** color image I

Output: An image with gray value I_{Gray}

Separate I in to 3 channel I_R, I_G, I_B

I_{Gray} = int8(I_R)+int(I_G)+int8(I_B)

Return I_{Gray}

Algorithm 4.1 Color Image to Grayscale Conversion Algorithm

4.4.2 Smoothing

There are various image filtering techniques that improve the quality of an image by reducing the paper and salt noise. These include adaptive median filtering, median filtering, wiener filtering,

image negation, histogram plotting and image subtraction. Out of these filtering methods, adaptive median filtering is more effective in image smoothening and preserves edges while removing noise like paper and salt. Therefore, in this thesis work, we applyied adaptive median filtering to improve the quality of microscopic urine image.

Adaptive Media Filtering: Adaptive Median Filter performs spatial processing to preserve detail and smooth non-impulsive noise. A prime benefit to this adaptive approach to median filtering is that repeated applications of this AMF do not erode edges or other small structures in the image. The main idea in the Adaptive Median Filter is to perform a spatial processing to determine which pixels in an image have been affected by impulse noise and run the filter only in this pixel. Then it classifies pixels as noise by comparing each pixel in the image to its surrounding neighbor pixels. That is a pixel different from the majority of its neighbors, as well as being not structurally aligned with those pixels is labeled as impulse noise. These noise pixels are then replaced by the median pixel value of the pixels in the neighborhood that have passed the noise labeling test. The size of the neighborhood is adjustable or threshold for the comparison. Figure 4.4 shows the result obtained after adaptive median filtering. Algorithm 4.2 shows adaptive median filtering algorithm

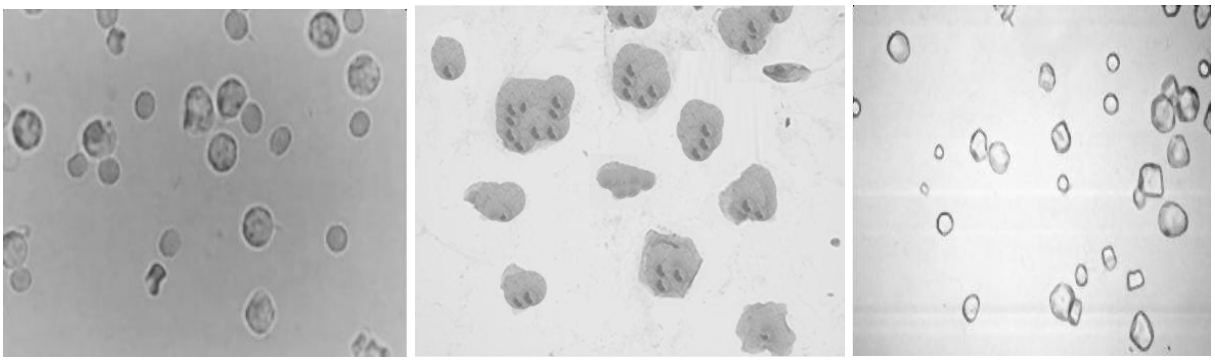

(A) (B) (C)

Figure 4.4: Grayscale Image after Applying Adaptive Median Filtering (A) White and Red Blood Cells, (B) Epithelial cell, (C) Crystal

In general, adaptive median filtering improves urine microscopic image by;

- removing salt-and-pepper (impulse) noise,
- provide smoothing of other noise, and
- reducing distortion.

```
Input: microscopic image
Output: preprocessed microscopic urine image
Choose window size Sxy
For shift window size one pixel down
   For shift window size one pixel right
           Get the minimum gray level in Sxy
           Get the maximum gray level in Sxy
           Get the median of gray levels in Sxy
           Get the gray level at coordinates (x,y)
           Get the maximum allowed size of Sxy
           A1   = zmed – zmin
           A2   = zmed – zmax
           If A1 > 0 and A2 < 0,
                Go to level B
           Else increase the window size
                If window size ≤ Smax
                    repeat level A
                Else
                    output zxy
   end
end
B:
           B1= zxy – zmin
           B2= zxy – zmax
           If B1 > 0 and B2 < 0,
                output zxy
           Else
                output zmed
```

Algorithm 4.2: Adaptive Median Filtering Algorithm

4.4.3 Image Adjustment

The grayscale image, after applying adaptive median filtering, is low contrast image to forward to the subsequent image processing techniques. Image adjustment adjusts intensity values of an image which basically involves intensity transformation so that the output image approximately matches to the predefine intensity. This predefined intensity value will increase the intensity value and produce high contrast image. Therefore, we apply intensity adjustment technique for mapping an image's intensity values to a new range. Figure 4.5 shows grayscale image after adjusting intensity value.

(A) (B) (C)

Figure 4.5: Image after Adjusting Intensity Values (A) White and Red Blood Cells, (B) Epithelial cell, (C) Crystal

4.5 Image Segmentation

This component responsible for division of an image into regions or categories, which correspond to different objects or parts of objects. Every pixel in an image is allocated to one of a number of these categories. The challenges while segmenting microscopic image is the occurrence of uneven illumination due to existence of light sources emitted from microscope. As a result, the rate of false detection will increase. In the thesis work, the segmentation is employed by integrating adaptive threshold and canny edge detection techniques.

4.5.1 Adaptive Threshold

Adaptive thresholding realizes the implementation of adaptive segmentation and is responsible to compensate non-uniformities illumination and reflection of microscopic urine image. Figure 4.6 shows the image after applying adaptive threshold. Algorithm 4.1 shows adaptive threshold.

(A) (B) (C)

Figure 4.6: Image after Adaptive Threshold (A) White and Red Blood Cells, (B) Epithelial cell, (C) Crystal

```
Input: preprocess microscopic urine image I
Output: foreground pixel
For each pixel location J in I
Get adaptive threshold T
  If I(J) > T
     I(J)=1
  Else
     I(J)=0
End
Return  I
```

Algorithm 4.3: Adaptive Threshold Algorithm

4.5.2 Canny Edge Detection

This sub component is responsible for detecting meaningful discontinuities in intensity values. Such discontinuities are detected by using first- and second-order derivatives. The edge detection operation is essentially an operation to detect significant local changes in the intensity level. The

basic idea behind Canny edge detection is to find places in an image where the intensity changes rapidly, using one of two general criteria:

- Find places where the first derivative of the intensity is greater in magnitude than a specified threshold.
- Find places where the second derivative of the intensity has a zero crossing.

Figure 4.7 shows the result after applying canny edge segmentation. Algorithm 4.2 shows after canny edge segmentation.

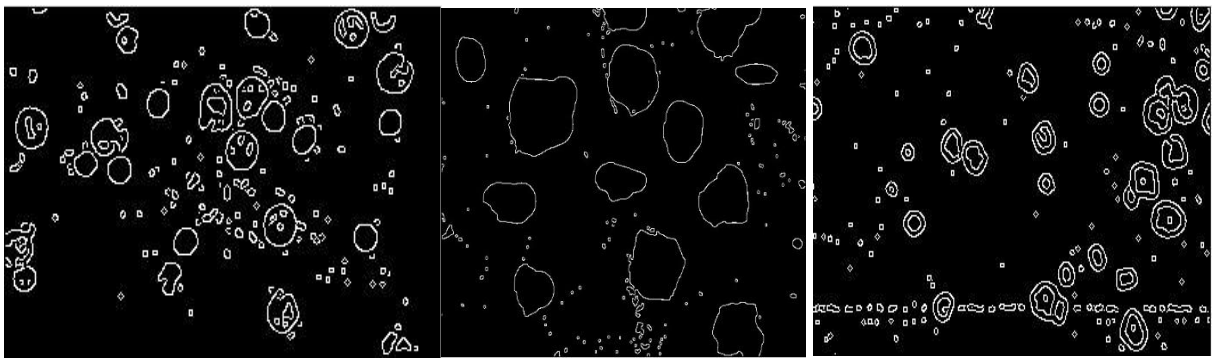

(A) (B)_ (C)

Figure 4.7 Image After Applying Canny Edge detection, (A) White and Red Blood Cells, (B) Epithelial cell, (C) Crystal

4.5.3 Fusion of Canny and Adaptive Thresholds Segmentation

After segmentation is applied using canny and adaptive thresholding, a further step should be done to give a hybrid result to render better segmentation result. Algorithm 4.3 shows hybrid canny edge detection and threshold segmentation algorithm.

Input: Segmentation result of adaptive thresholding: $\mathbf{S_{adaptive}}$, Segmentation result of canny edge detection: **C**

An image of **I** where size(I)=size($\mathbf{S_{adaptive}}$) and $I(_{i\ ,\ j})=0$

Output: Segmented result **I**

```
FOR each I= 1: size(I,1)
    FOR each J= 1: size(I,2)
        IF (S_adaptive(I,J) == (C(I,J)  AND S_adaptive(I,J)==1))
```

```
                I(I,J) = 1
            END IF
        END FOR
    END FOR
    Apply morphological erosion followed by dilation on I
    Return I
```

Algorithm 4.4: Hybrid Canny Edge Detection and Threshold Segmentation Algorithm

4.5.4 Morphological Operation

Furthermore, morphological operations are also applied to fill and remove tiny objects. The image should be represented as a boundary or as a complete region. This refers to certain operations where an object is hit with a structuring element and thereby reduced to more revealing shape. To create a structuring element of the cell or to detect the exact shape of cells, further morphological operation is crucial to get a better result. Morphological operation including erosion and dilation has been applied to eliminate small unwanted pixel and image smoothing. The erosion operation uniformly reduces the size of objects in relation to their background and dilation expands the size of objects. Besides dilation and erosion, secondary operations like opening and closing can be applied on the image. Figure 4.8 shows after applying morphological operation. Figure 4.9 shows Microscopic, Binary and Grayscale Segmentation.

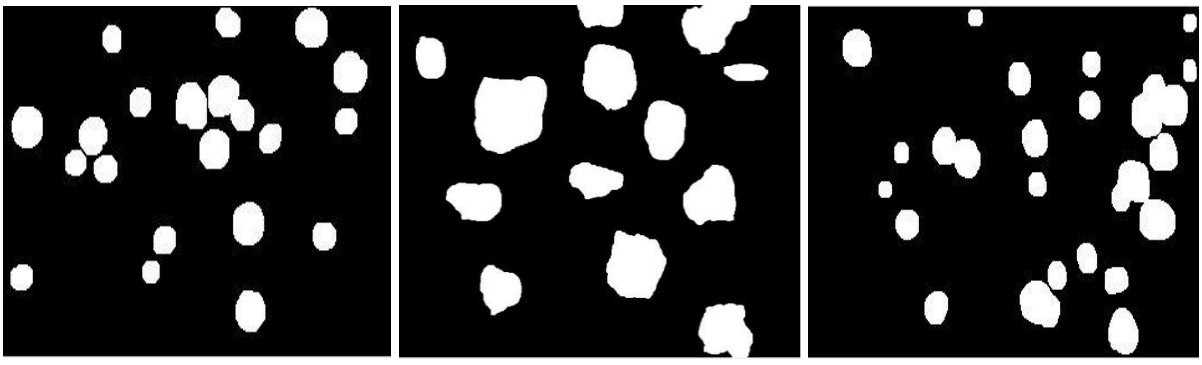

(A) (B) (C)

Figure 4.8: Image after Applying Hybrid of Canny, Adaptive and Morphological Operation, (A) White Blood Cells, (B) Epithelial cell, (C) Crystal

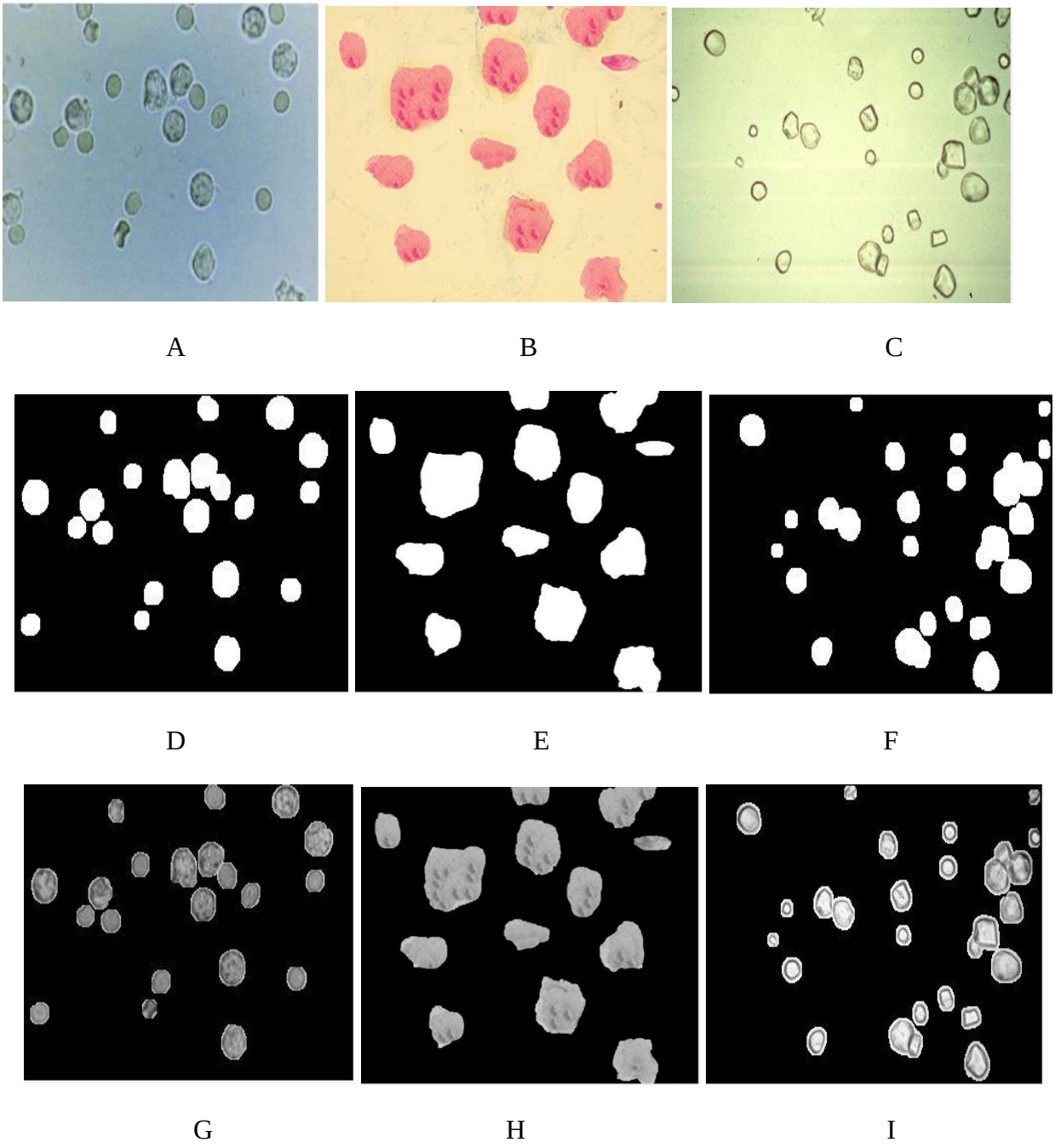

Figure 4.9: Microscopic Image (A) WBC and WBC, (B) EP, (C) Crystal, Binary Segmentation (D), (E) and (F) and Grayscale Segmentation (G), (H) and (I)

4.6 Feature Extraction

This section aims for extracting features that are used to describe sediments in urine micrograph. As discussed in the literature review section, the major goal of feature extraction is to extract a set

of features, which maximizes the recognition rate with the least number of elements and to generate similar feature set for variety of instances of the same symbol. Images have different features like geometric, texture and color features. These features are used to represent or identify an object in an image. We used geometric, texture and color features to represent sediments in urine since different shape, statistical texture and HSV color are represented sediment in urine. On the other hand, one suspended sediment cannot have identical color due to microscope control adjustment and chemical used in the preprocess stage. So, we used HSV color feature extraction method in addition to adaptive threshold segmentation techniques. Therefore, in this research, geometric, statistical texture and color feature are used to model sediments in urine microscopic image.

4.6.1 Texture Feature Extraction

Texture is an important property of image and powerful regional descriptor that helps in the retrieval process. Statistical, structural, and spectral are the three principal approaches used in image processing to describe the texture of the region. Among the three principal approaches we used statistical feature to analyze the texture of the sediment. Statistical texture measures the arithmetic mean of the intensity value, standard deviation, third moment, uniformity, and entropy of the interest region. These are calculated as follows. Let us consider x_i as a discrete random variable that corresponds to the intensity levels of an image and let us denote $p(x_i)$ as the corresponding normalized histogram, with i = 0, 1, 2, … , L-1 and L is the number of possible intensity values [45].

Arithmetic mean: The arithmetic mean of a set of intensity values is the ratio of their sum to the total number of intensity values in the set. Thus, if there are a total of *n* numbers in a data set whose values are given by a group of *x*-values, then the arithmetic mean of these values, represented by μ, can be found as:

$$\mu = \frac{1}{n}\sum_{i=1}^{n} x_i \tag{15}$$

Variance: is a measurement of the spread between numbers in a data set. It measures how far each number in the set is from the mean. Variance is calculated by taking the differences between each number in the set and the mean, squaring the differences and dividing the sum of the squares by the number of values in the set. It can be calculated using Equation 16.

$$\sigma 2 = \frac{1}{n-1}\sum_{i=1}^{n}(x_i - \mu) \quad (16)$$

Standard deviation: is the measure of dispersion of a set of data from its mean. It measures the absolute variability of a distribution; the higher the dispersion or variability, the greater is the standard deviation and greater will be the magnitude of the deviation of the value from their mean. It can be calculated using Equation 17

$$\sigma = \sqrt{\frac{1}{n-1}\sum_{i=1}^{n}(x_i - \mu)} \quad (17)$$

Smoothness: Measures the relative smoothness of the intensity in a region (R). Calculate smoothness or Roughness Region surface. R = 0, the surface intensity is flat or homogeny region. R approaches 1, the surface of the region is rough or has variations in intensity or high contrast. It can be calculated using Equation 18.

$$R = 1 - \frac{1}{1+\sigma^2} \quad (18)$$

Third moment: Measures the skewness of a histogram. If the histogram is symmetric than $\mu_3 = 0$, if it is skewed to the right of the mean than $\mu_3 > 0$, and if it is skewed to the left of the mean than $\mu_3 < 0$. Values of this measure are brought into a range of values comparable to the other five measures by dividing μ_3 by $(L-1)^2$. It can be calculated using Equation 19.

$$\mu 3 = \sum_{i=0}^{L-1}(x_i + \mu)^3 p(x_i) \quad (19)$$

Uniformity: uniformity measure is maximum when all intensity values are equal (maximally uniform) and decreases from there. It can be calculated by using Equation 20.

$$u = \sum_{i-1}^{L=1} p^2(x_i) \quad (20)$$

Entropy: A measure of randomness. It can be calculated using Equation 21.

$$e = \sum_{i-1}^{L=1} p^2(x_i)\, log_2 p(x_i) \quad (12)$$

4.6.2 Geometric Feature Extraction

Geometric feature is one of the most important features to represent the spatial distribution of pixels. As discussed in the literature review section the contour methods calculate feature from the boundary and ignore its interior, while the region methods calculate feature from the entire region. In this research, we used the combination of contour and region-based feature extractions methods to model sediment in urine microscopic image [30].

Among the most important geometric features, area, perimeter, major axis length, minor axis length, Orientation aspect ratio and eccentricity are the six features used from both contour and region-based feature extractions methods to analyze the morphology of the particle in urine image. These are described as follows.

Minor Axis Length: Number of pixels between the extreme points of longest line along the width of the sediments.

Major Axis Length: Number of pixels between the extreme points of shortest line along the width of the sediments.

Eccentricity: The eccentricity is calculated by fraction of the number of pixels between the major axis length and foci of the ellipse. The value of eccentricity is between 0 and 1.

Perimeter: Total number of pixels which makes the boundary of the sediments

Area: Total number of pixels in the segmented sediment.

Orientation: The angle between horizontal axis and major axis.

Aspect Ratio: It is the major axis length divided by minor axis length.

4.6.3 Color Feature Extraction

HSV is an alternative representation of the RGB color. In HSV, color is described by three components: hue, saturation and value (intensity). In these models, colors of each hue are arranged in a radial slice, around a central axis of neutral colors which ranges from black at the bottom to white at the top. The HSV representation models the way paints of different colors mix together, with the saturation dimension resembling various shades of brightly colored paint, and the value dimension resembling the mixture of those paints with varying amounts of black or white paint. The color features for sediment are obtained by converting RGB into HSV [23].

The feature space therefore is composed of the following attributes: the mean, standard deviation, the median and the range of hue, saturation and value of the color model. Three color features extracted from each component hue, saturation and value.

4.6.4 Feature Fusion

Although it is possible to extract a large set of features, only a small subset of them is used in the classification due to the course of dimensionality and variant. In addition, some features have no strong correlation with other features. Therefore, there is an incentive to combine small subset of features, which is the most proper representations, to produce a feature vector that maximizes the recognition rate. The features vector is grouped into geometrical, texture and HSV categories based on the information they provide. The geometrical feature provides information about area, perimeter, diameter, major axis length, minor axis length and eccentricity. The texture feature provides information about mean, variance, standard deviation, third moment, entropy and smoothness. The color future provides information about hue, saturation and value. A total of twenty-three feature vectors are extracted from each sediment in the microscopic urine image.

4.4 Classification

The area expert labels each object presented in the urine microscopic image and the labeled image is pre-processed, segmented and seven geometrical, seven texture and nine color features are extracted using image analysis technique. The next phase is identifying WBCs, RBCs, Eps and crystal which are observed in microscopic urine image based on a set of known tags or features.

Since we have a labeled data, we used machine learning method to identify the class of the image. The classification tasks are supervised learning in the sense that the algorithms need ground truth information or class label or category information to build or train the model. Once the training is done on ground truth data, the model can be used to predict data which the model has never seen before. We have chosen multiple support vector machine and neural network for this task. MSVM is a very effective method for classification and general pattern recognition. In addition, its high generalization performance without the need to add a priori knowledge, even when the dimension of the input space is very high. Neural network has favorable properties that make it an excellent choice for object classification. These include generalization, expandability, representing multiple samples, and memory saving.

In the case of ANN, we need to select optimum architecture (topology) and training algorithm that best matches to the proposed classification model. In our study, feed forward multi-layer perceptron (MLP) architecture is used. It is composed of three types of layers: input layer, output layer and hidden layer. The combination of geometric, texture and color features that we have computed in the previous section are used as an input layer which has 25 neurons. Based on these selected features, the number of hidden layers is 50, as a result NN gives us 4 generated output classes, i.e., WBC, RBC EP and Crystal. Figure 4.10 shows multilayer perceptron neural network model and Figure 4.11 shows the final generated model of NN.

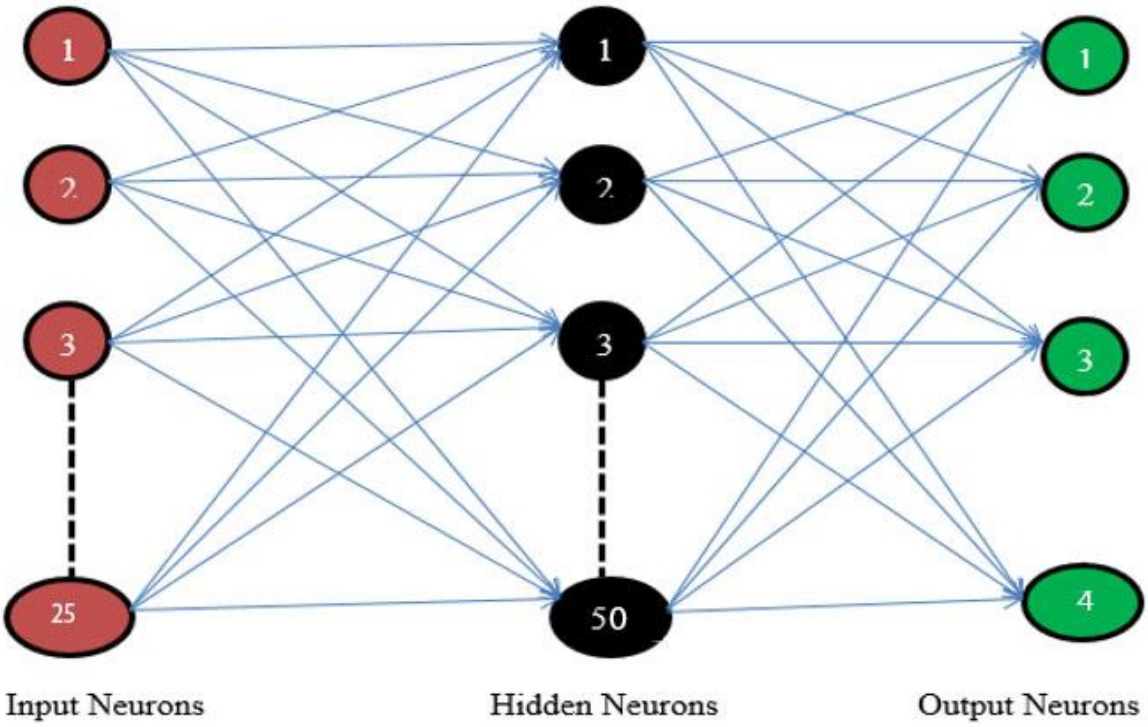

Figure 4.10: Multilayer Perceptron Network Model

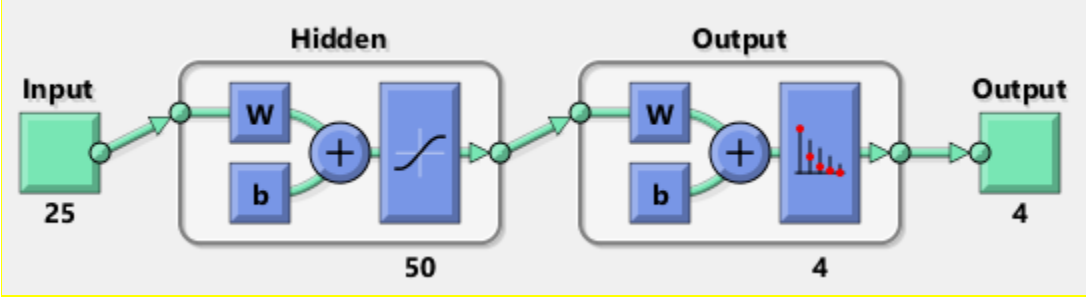

Figure 4.11: Final Generated Model of NN

To build a model using SVM which is basically binary classifier, we applied a multi class SVM classifier since the expected outputs generated from our model have more than two classes as shown in Figure 4.12. Though, there are various multi-class SVM with kernel functions which are used to construct a model for classifying sediments inside the urine, with all radial basis function is found to be better classifier to identify sediments inside the urine.

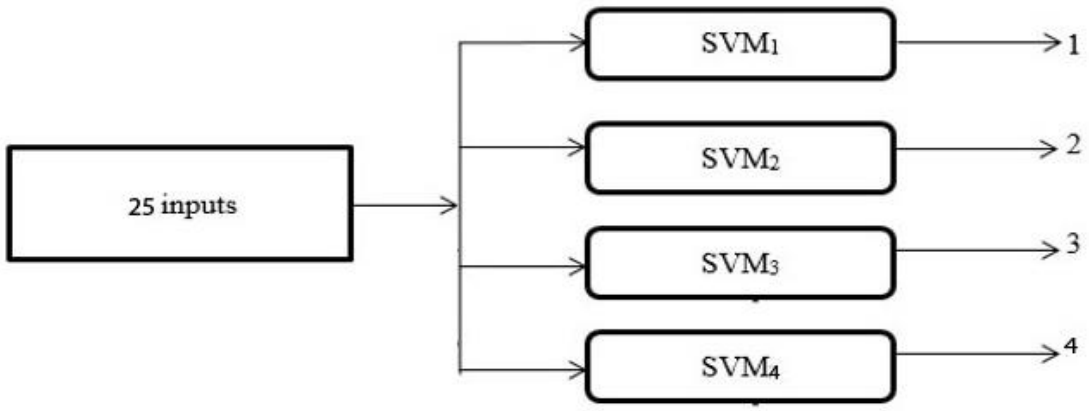

Figure 4.12: Multi-Class Support Vector Machine Network Model

4.5 Summary

In this chapter, the design of automatic sediment detection system in urine based on image processing technique is discussed. The proposed system consists of two main phases: training and classification. In the first phase, urine microscopic images are used to create knowledge base. During the creation of the knowledge base, images are pre-processed using adaptive median filtering, image adjustment and medial filtering technique. Then images are segmented using a combination of canny edge detection and adaptive technique to differentiate sediments in microscopic urine image. Consecutively, twenty-three features which are combinations of geometric, texture and color are extracted to represent or identify classes of sediments in urine. Finally, an artificial neural network and multiclass support vector machine model are used to train input features extracted from the individual segmented image to represent the knowledge base. In the second phase, knowledge base is used to identify the classes of sediments.

CHAPTER FIVE: EXPERIMENTAL RESULTS

5.1 Introduction

In this Chapter, experimental evaluation of the proposed architecture is conducted to evaluate the performance of the system. Evaluating performance is an important and integral part of any system. It helps to find the best model that represents our data and how well the chosen model will work in the future. Thus, to conduct the experiment, dataset was collected from standard medical image databases that are used for research purpose and prototype was developed to demonstrate the usability of the system. Finally, the overall experimenting process is discussed.

5.2 Dataset

The evaluation was conducted using images collected from standard medical image databases that are used for research purpose and image taken from microscopic image. In both cases, the data sets were taken from drop of suspended sediment is poured onto a glass slide using a camera-mounted in microscope along with a computer under different control environments.

Dataset are taken from Masaryk University database which is used for research purpose. Dataset are also captured using Leica DM750 HD Camera mounted on microscope at Addis Ababa University, college of Medicine, Department of Pathology. Table 5.1 shows data description.

Table 5.1: Data Description

Serial.No	Source	Image format	Image Quantity	Particle in image
1	Masaryk University	jpeg	110	1260
2	Addis Ababa University	jpeg	30	320

One hundred forty urines microscopic images, which incorporate at least WBCs, RBCs, Eps and crystal were collected. Accordingly, we have created our own dataset that contain four different classes. From the total of 1580 dataset 1422 were used for training and 158 were used for testing.

5.3 Implementation

We used MATHLAB 2017a to implement the prototype. MATLAB is a scientific programming language and provides strong mathematical and numerical support for the implementation of advanced algorithms. We used Windows 7 64-bit operating system, intel® Core ® i7-6700HQ CPU @ 2.60GHz, 2592 MHz, 4 Core(s), 8 Logical Processor(s) Processor, and intel® HD graphic 530 HP laptop is used in this research. Figure 5.1 the graphical user interface of the developed prototype.

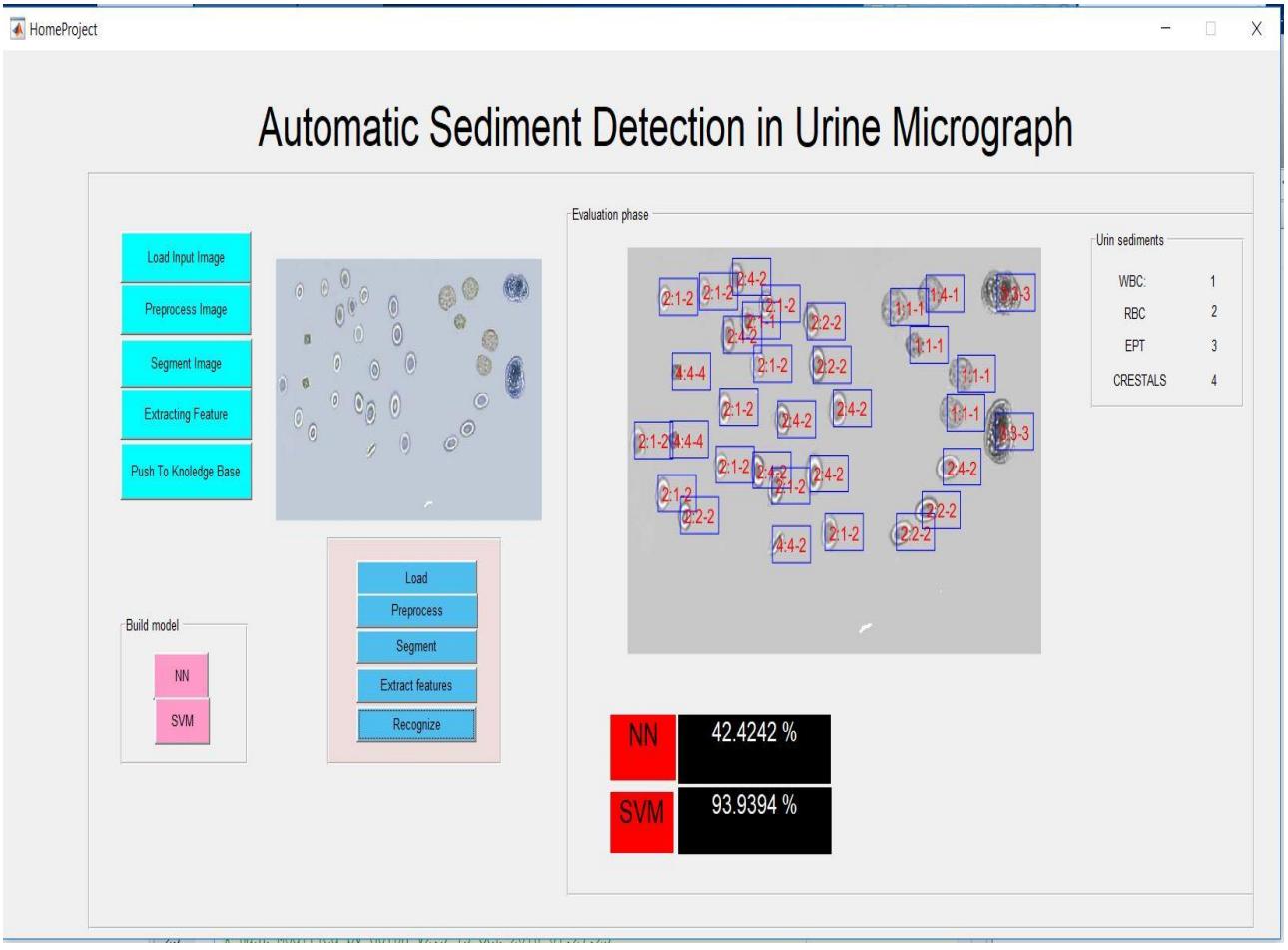

Figure 5.1: Screenshot of the User Interface of the Developed Prototype

5.4 Evaluation

Evaluating machine learning algorithm is an essential part of any project. The basic principle of machine learning is to build algorithms that receive input data and analyses to predict an output.

Simply splitting the microscopic image dataset into a single training and testing set may not give the best estimate of future performance. Therefore, we use cross validation to validate the stability of our machine learning model and a confusion matrix to describe the performance of a classification model.

We used 10-fold cross-validation to minimize overoptimistic result and to maximize accurate performance estimation. First, we partitioned 1580 dataset into ten equal sized folds which is 158. Subsequently ten iterations of training and validation are performed sequentially. Within each iteration, one-fold of the data is held-out for validation while the remaining nine-folds are used for learning.

To evaluate the performance, we used four performance matrices to analyze the classification performance of NN and SVM models. These performance matrices are: accuracy, recall, precision and specificity. All of them are calculated from the number of objects relevant to the query determined by method. Based on this, we define accuracy (A) as the number of correctly predicted sediments to the total number of sediments. Precision is the ratio of correctly predicted positive observations to the total positive predicted observations. Recall is Recall is the ratio of correctly predicted positive observations to total number of positive observations. These performance evaluation criterions were based on the number of true positives (TP), true negatives (TN), false positives (FP), and false negatives (FN). All these parameters are given by the following Equations 9, 10 and 11 respectively:

$$Accuracy = \frac{TP+TN}{TP+FN+FP+TN} \tag{22}$$

$$Pr\,cision = \frac{TP}{TP+FP} \tag{23}$$

$$Recall = \frac{TP}{TP+FN} \tag{24}$$

$$Specificity = \frac{TN}{TN+FP} \tag{25}$$

A true positive (TP) is when the classifiers correctly predict the sediments as a part of correct class and a true negative (TN) is when the classifier correctly predicts the sediments as not part of a correct class. A false positive (FP) occurs when a classifier incorrectly classifies the sediments;

but they are in the class and false negative (FN) occurs when the classifier incorrectly classified the sediment as a part the incorrect class.

The result of accuracy and recall, precision and specificity for SVM and NN models is presented in Tables 5.2, and 5.3 respectively. All standard metrics for measuring the performance of the system are evaluated from the value ten confusion matrixes. We illustrated the first confusion matrix of NN and SVM as an example in Figure 5.3.

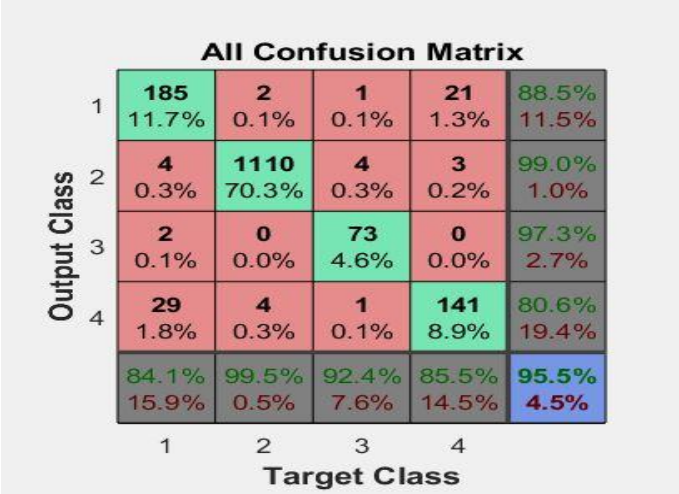

158	1	2	3	4		
1	17	0	2	1		20
2	1	125	0	0		126
3	2	0	4	1		7
4	0	1	0	8		9
	20	126	6	10		0.974684

(a) Neural Network (b) Multiple Support Vector Machine

Figure 5.2: Confusion Metrics for the First-Fold in NN and SVM

Table 5.2: NN and SVM Model Accuracy Result

Experiment	**Fold-1**	**Fold-2**	**Fold-3**	**Fold-4**	**Fold-5**	**Fold-6**	**Fold-7**	**Fold-8**	**Fold-9**	**Fold10**	**Avg (%)**
Accuracy-NN (%)	95.50	97.30	98.00	95.10	96.50	96.70	95.40	94.80	94.10	95.90	**95.93**
Accuracy-SVM (%)	97.46	95.56	98.73	98.74	97.47	94.30	98.10	97.46	98.73	97.45	**97.40**

As seen in Table 5.2, we found that the recognition accuracy for Neural network is 95.50%, 97.30%, 98.00%, 95.10%, 96.50%, 96.70%, 95.40%, 94.80%, 94.10% and 95.90% on each experiment. The lowest and the highest recognition accuracy for NN is 94.10% and 98.00%. The average recognition accuracy for NN is 95.93%. In support vector machine the recognition accuracy is 97.46%, 95.56%, 98.73%,98.74 %, 97.47%, 94.30%, 98.10%,9 97.46%, 98.73 and 77.45% for each experiment. For SVM, the lowest recognition accuracy is 94.30% and the highest recognition percentage is 98.73% recorded. The average recognition accuracy from those experiments is 97.40%. The recognition accuracy results of NN and SVM models is illustrated with a bar chart presented in Figure 5.3.

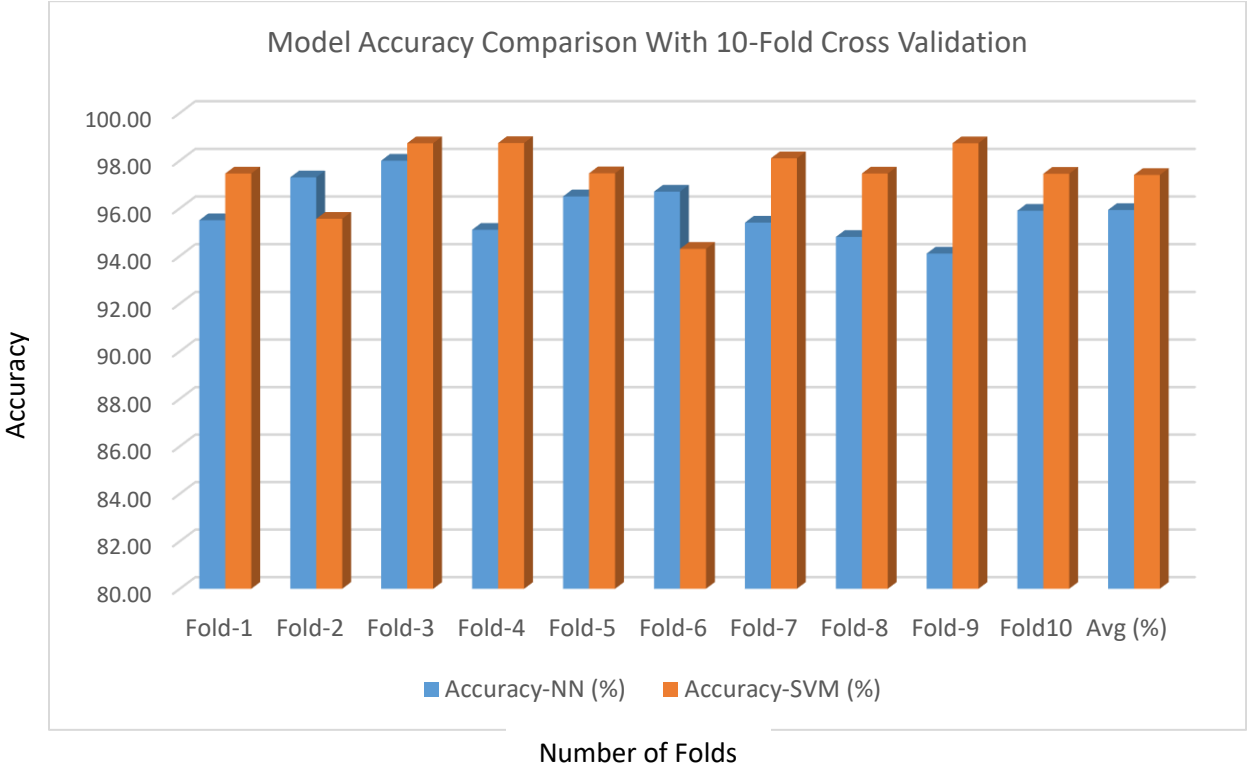

Figure 5.3: NN and SVM Classification Accuracy Results with Bar Chart

Table 5.3: Other Performance Measure for NN and SVM

Evaluation matrix	Model	Class			
		WBC %	RBC %	EP %	Crystal %
Recall	**NN**	87.89	97.54	97.54	88.38
	SVM	93.01	98.47	79.31	90.59
Precession	**NN**	85.98	98.65	87.77	88.46
	SVM	91.28	98.17	100.00	77.27
Specificity	**NN**	97.51	96.95	99.27	98.66
	SVM	99.26	96.23	100.00	96.53

The recall of WBC, RBC EP and Crystal in neural network model were 87.89%, 97.54%, 97.54%, and 88.38% receptively. Which means out of all WBC class, 87.89% of the images were correctly predicted, out of all RBC class, 97.54% of the images were correctly predicted, out of all EP class 97.54% of the images were correctly predicted, out of all Crystal class, 88.38% of the images were correctly predicted. In support vector machine model, the recall WBC, RBC EP and Crystal was 93.01%, 98.47%, 79.31% and 90.59% receptively. This means out of all WBC class, 93.01% of the images were correctly predicted, out of all RBC class, 98.47% of the images were correctly predicted, out of all EP class, 79.31% of the image were correctly predicted, out of all Crystal class, 90.59% of the images were correctly predicted.

The precision value of WBC, RBC EP and Crystal in neural network model were 85.98%, 98.65%, 87.77%, and 88.46% receptively. Which means, WBC class was predicted, 85.98% of the time the system was in fact correct, For RBC class, 98.65% of the time the system was in fact correct, For EP class, 85.98% of the time the system was in fact correct, For Crystal class, 88.46% of the time the system was in fact correct. In Support Vector Machine the precession value of WBC, RBC EP and Crystal were 85.98%, 98.65%, 87.77%, and 88.46% receptively. Which means, WBC class was predicted, 85.98 % of the time the system was in fact correct, For RBC class, 98.65 % of the time the system was in fact correct, for EP class, 85.98 % of the time the system was in fact correct, for Crystal class, 88.46 % of the time the system was in fact correct.

The specificity value the WBC, RBC EP and Crystal in neural network model the was 97.51%, 96.95%, 99.27%, and 98.66% receptively. Which means a probability that a non-detected WBC image was not an WBC is 97.51%, a probability that a non-detected RBC image was not an RBC is 96.95%, a probability that a non-detected EP image was not an EP is 98.66% and a probability that a non-detected Crystal image was not Crystal is 98.66%. In Support vector Machine model, the specificity value the WBC, RBC EP and Crystal was 99.26%, 96.23%, 100%, and 96.53% receptively. Which means a probability that a non-detected WBC image was not an WBC was 99.26%, a probability that a non-detected RBC image was not an RBC is 96.23%, a probability that a non-detected EP image was not an EP is 100%, and a probability that a non-detected Crystal image was not Crystal is 96.53%.

5.5 Discussion

The proposed sediment detection and classification system is evaluated from the capability of learning machines (SVM and NN) to recognize sediment into its corresponding class based on features. Learn-ability of the selected learning machines is evaluated by ten iterative training and testing dataset. Within each iteration 90% of the dataset are used for training while the remaining 10% are used for testing.

Out of all classes of sediment 98.47% of the RBC were correctly predicted in MSVM classifier, 100% of the time the system correctly predicted EP in MSVM classifier, a probability that a non-detected EP is not an WBC is 100% in MSVM classifier and MSVM recognition accuracy is 97.40%. Therefore, in this research MSVM has a very good performance even though it uses more memory then NN. We believe that the problem of speed and memory may not be a serious problem for detection and classification of urine sediment because in the health care industry the fundamental concern is accuracy. From this perspective, MSVM classifies better than NN regardless of its high memory usage.

Accordingly, the proposed technique demonstrated acceptable detection performance. The performance of the proposed prototype is found to be effective for the identification of sediments in urine sample even in the context where sediments in urine have irregular shape, different color and poorly illuminated microscopic images.

CHAPTER SIX: CONCLUSION AND FUTURE WORKS

6.1 Conclusion

In this study, an attempt has been made to implement a system which is capable of detecting and classifying sediments in urine microscopic image. The system two phases, i.e., training and classification. The first phase has four main parts: Image preprocessing, segmentation, feature extraction and model creation. The classification phase also four parts: Image preprocessing, segmentation, feature extraction and classification. The first three parts are identical in both phases which is responsible for division of an image. Model creation is responsible for creating knowledge database and classification is responsible for classing sediment to the respective type

In the first part microscopic urine images are collected from standard medical image databases that are used for research purpose and image is also capture using a camera-mounted in microscope under different control environment. Then set of sequential preprocesses such as smoothing, creating gray scale image, enhancing and segmented image is applied to improve the quality of an image by reducing the paper and salt noise. After preprocessing, hybrid image segmentation technique is applied, which is the combination of canny edge detection and adaptive thresholding, to segment and improve illumination problem. A total of twenty-three features that are best suited to represent the sediment in the microscopic urine image are extracted from shape, texture and color sediment. Those twenty-three features are used to create the knowledge base which is used to train an artificial neural network and multiple support vector machine. Finally, 10-fold cross validation and confusion matrix were applied to examine the efficiency and the performance of the system. The performance of each model is compared using tenfold cross validation and we obtained an acceptable detection performance.

Accordingly, a system for detecting and classifying sediment in urine microscopic image using image processing technique was developed. The gaps for manual sediment detection specifically dependent on the skill, experience and motivation of the technician mandated for the task was solved. The use of an automated digital microscope urine image, which would allow entire slides to be examined, would allow the system to make diagnoses with a high degree of certainty.

In conclusion, our developed prototype that detects and classifies microscopic urine image has a very good performance in four evaluation matrices and the implementation of this work in real situation will be advantageous it produces a result which is closer to what an expert does.

6.2 Contribution of the Thesis

As a contribution, the proposed system offered a systematic approach in the process of automatic detection and classification of sediment in urine microscopic image. In preprocessing activity, the combination of adaptive media filtering and image adjustment are employed which is effective in image smoothening and preserving edges while removing noise. Considering segmentation, we proposed hybrid approaches of canny and adaptive threshold to improve the occurrence of uneven illumination problem which is due to the existence of light sources emitted from microscope and external source. In this regard, a total of twenty-three features are extracted from shape, texture and color of microscopic urine image to represent sediments in urine. Finally, we proposed neural network and multi class support vector machine models to measure the performance of the system. Therefore, the following are the contributions.

- A hybrid segmentation algorithm has been developed to segment urine microscopic image that is affected by poor illumination.
- A fused feature extraction technique has been produced to represent sediments in urine microscopic image.
- A method for successful detection and classification of sediment has been made possible.
- A hybrid segmentation approach that is a combination of canny and adaptive threshold has been made possible.
- A unified model that detects and classifies sediments in urine microscopic image has been developed.

6.3 Future Work

In this thesis, we attained a result in detecting and classifying microscopic urine image. It has its own impact on automatic detecting sediments in urine. In the process of data collection, a lot of challenges have faced, for instance, to address this some of the images are highly affected by

illumination which could make the segmentation process more complex. To address this challenge, we applied adaptive thresholding and canny segmentation followed by morphological operation. However, there are gaps which should be filled in the future. The following are some of the future works.

- This work using multiple support vector machine has a good evaluation result for detecting and recognition of WBCs, RBCs, EPs and Crystal in urine microscopic image. Thus, extending this work to other remaining sediment such as cast and artifact.
- In this research work, the main challenge was obtaining enough microscopic urine image. So, we capture all the remaining necessary image. There should be other database that includes all sediment in urine. This will significantly increase the performance of the system.

Reference

[1] X B. Song, J Sill, Y. Abu-Mostafa, and H. Kasdan, *Image Recognition in Context Application*, Oregon Graduate Institute of Science and Technology, California Institute of Technology, 2011.

[2] N. Ieiri, O. Hotta, and Y. Taguma, "Impact of Annual Urine Health Checkup System to Obtain Clinical Remission in Patients with IGA Nephropathy," *Contrib. Nephron*, Vol. 157, 2007, pp. 104-108.

[3] Rai A.J, *The Urinary Proteome Methods and Protocols*, New York, NY: Humana Press, 2010.

[4] Yingchun Li, Guangda Su, and Zhanchun Li, "Detecting Particle Objects in Image," *International Journal of Information Technology*, Vol. 11, No. 7, 2005, pp. 178-186.

[5] Hongwen Luo, Siliang Ma, and Danyang Wu, *Mumford-Shah Segmentation for Microscopic Image of the Urinary Sediment*, College of Mathematics Jilin University Changchun, 2009.

[6] Yingchun Li, Guangda Su, and Zhanchun Li, "Automatic Detecting Particle Objects in Image," *International Journal of Information Technology*, Vol. 11, No. 7, 2005, pp. 39-49.

[7] Guitao Cao, Cai Zhong, Ling Li, and Jun Dong, *Detection of Red Blood Cell in Urine Micrograph*, *International Journal of Information Technology,* Vol. 4, No. 6, 2009, pp. 144-156.

[8] A Yan Zhou and Houkui Zhou, Automatic *Classification and Recognition of Particles in Urinary Sediment Images Computer*, 2012.

[9] Almadhoun, M.D, "Automated Recognition of Urinary Epithelial cells," *paper presented at the International Conference on Technological Advances in Electrical, Electronics & Computer Engineering*, Konya, 2013.

[10] Microscopic Urine Sample Images, "Microscopic Analysis of Urine Faculty of Medicine, Masaryk University_files," white paper, 2010, retrieved from http://www.meddean.luc.edu/lumen/MedEd/medicine/PULMONAR/Renal/Atlas/urineatlas_f.htm, Last accessed on June , 2018

[11] Xue-Qin, Yang, Bin Fang, and Jun-Feng Xiong, "An Efficient Casts Recognition Algorithm in Urinary Sediment Image," in *Proceedings of the International* Conference *on Multimedia*, China, June 10, 2010.

[13] Chan-Yan Li, Bin Fang, Yi Wang, Guang-Zhou Lu, Ji-Ye, and Qien, Lin Chen, "Automatic Detection and Recognition of Cast in Urine Sediments," in *Proceedings of the International Conference on Wavelet Analysis and Pattern Recognition*, Chongqing, China, July 2009

[14] M. Mausumi, G. Rahul, and M. Mukherjee, "Detection and Counting of Red Blood Cells in Blood Cell Images using Hough Transform," *International Journal of Computer Applications,* Vol. 53, No. 16, 2012, pp. 18-22.

[15] Kiran Tiwari, and Pooja Thakre, "An Efficient Approach to Track RBC and Detect Blood Disease using Blood Samples," *International Journal of Science Technology and Engineering*, Vol. 2, No. 10, 2010.

[16] Karen M. Ringsrud, "Cells in the Urine Sediment laboratory medicine," *ASCP,* Vol. 32, No. 3, March 2000.

[17] Sumeet Chourasiya and Ashish Goud Purushotham, *Review on Automatic Red Blood Cell Counting*, Department of Electronics and Communication Engineering Jagadguru Dattatray College of Technology, India, 2014.

[18] Mohamed D. Almadhoun, *Optimum Automated Procedures for Detecting and Mining Microscopic Urine Particles*, 2002.

[19] Education Commentary Red Blood Cell and White Blood Cell in Urine Urinalysis, American Proficiency Institute, 2014.

[20] Microscopic Urine Sediments Sample Images, "Microscopic Analyses of Urine Sedimnets," retrieved from https://allhealthpost.com/crystals-in-urine/, Last accessed on May 20, 2018.

[21] Ming-Hsuan Y., Kriegman D., and Narendra, "A Detecting Faces in Images A Survey," *Institute of Electrical and Electronics Engineers,* Vol. 24, 2002, pp. 34-58.

[22] Zhang Y.J., "Evaluation and Comparison of Different Segmentation Algorithms, Pattern Recognition Letter," *International Journal of Information Technology,* Vol. 18, 1997, pp. 963-974.

[23] Rafael C. Gonzalez Richard, and E. Woods, *Digital Image Processing 3rd Edition*, New Jersey, 2008.

[24] XueMei Liu, ZhiJian Sun, "A Kind of Computer Microscopic Urinary Sediments Analyzer by SVM," *Institute of Electrical and Electronics Engineers*, Vol. 2, 2008, pp. 34-36.

[25] Daniel Zemene Mequanint, "Automatic Malaria Detection from Images of Microscopic Thin Blood Films," Unpublished Masters Thesis, Department of Computer Science, Addis Ababa University, 2016.

[26] SHEN Mei-li and Zhang Rui, *Urine Sediment Recognition Method Based on SVM and AdaBoost*," 2009.

[27] Joaquim Jose Furtado, Zhihua Cai, and Liu Xiaobo, *Digital Image Processing Supervised Classification Using Genetic Algorithm in MATLAB Toolbox*, 2010.

[28] Y.Murasaki, K.Tanigiichi, and Y.Murakami, "Pattern Recognition of Urinary Sediment Images Applying a Fuzzy-neural Network", *Trans of Inclusive Early Childhood Education*, Vol.76, No. 12, 2003, pp. 2630- 2632.

[29] Jain LC and Vemuri VR, *Industrial applications of neural networks*, CRC press, New York, 2009.

[30] Rafael C. Gonzalez,Richard E. Woods, E.Steven L and Eddins Woods, *Digital Image Processing Using MATLAB*, Gatesmark Publishing, 2009.

[31] Rajkumar Goel, Vineet Kumar, Saurabh Srivastava, "A. K. SinhaA Review of Feature Extraction Techniques for Image Analysis," *International Conference on Advances in Computational Techniques and Research Practices Noida Institute of Engineering & Technology*, Vol. 6, Special Issue 2, 2017, pp. 179-186.

[32] Sudhir M. Gorade, Prof. Ankit Deo, Preetesh Purohit, "A Study of Some Data Mining Classification Techniques," *International Research Journal of Engineering and Technology (IRJET)*, Vol. 04, April 2017, pp. 200-210.

[33] B. Kiranmai, and A. Damodaram, "Review on Evaluation Measures for Data Mining Tasks," *International Journal Of Engineering And Computer Science*, Vol. 3, 2014, pp. 217-220.

[34] “Data Science Central Community Channels devoted entirely to all things Data Viz” retrieved from https://www.datavizualization.datasciencecentral.com, Last accessed on August 26, 2018.

[35] Nasrul Humaimi Mahmood and Muhammad Asraf Mansor, “Red Blood Cells Estimation Using Hough Transform Technique,” *An International Journal,* Vol.3, No.2, April 2012.

[36] S. Pavithra and J. Bagyamani, “White Blood Cell Analysis Using Watershed and Circular Hough Transform Technique,” *International Journal of Computational Intelligence and Informatics,* Vol. 5: No. 2, September 2015.

[37] Manisha Shirvoikar and.H.G.Virani, “Detection and Segmentation of WBC Cells Using Image Processing Technique,” *International Journal of Technology and Science,* Volume 5, No. 1, 2016, pp. 56-58.

[38] Ying-Chun Li, Zhan-Chun Li, Yun-Huan Mei, and Jian-Xin Zhang, "Detecting Algorithm Based Gabor in Microscopic Image", *Proceedings of the Fourth International Conference on Machine Learning and Cybernetics, Guangzhou,* August 2005.

[39] Chun-Yan li, Bin Fang, Yi Wang, Guang-Zuang Lu, Ji-Ye Qian, L and in Chen, “Automatic Detection and Recognition of Casts in Urine Sediment Image,” *in Proceedings of the 2009 International Conference on Wavelet Analysis and Pattern Recognition,* Baoding, July 2009.

[40] Luo, T., Kramer, K., Goldgof, D.B., Hall, L.O., Samson, S., Remsen, and A.,Hopkins, T., “Recognizing Plankton Images From the Shadow Image Particle Profiling Evaluation recorder,” *Institute of Electrical and Electronics Engineers* Transactions on System, Man and Vol. 34, No. 2, 2004, pp. 153-1762.

[41] Uebele, Abe and S. Lan, “A neural-network-based fuzzy classifier” Institute of Electrical and Electronics Engineers Transactions, Vol. 25, No. 2, pp. 153-361.

[42] Ronneberger, O., Heimann, U., Schultz, E., Dietze, V., Burkhardt, H., and Gehrig R., Automated Pollen Recognition Using Gray Scale Invariants on 3D Volume Image Data, 2000.

[43] Ning Feng ZENG, Keiji TANIGUCHI, SadakazuWATANAEIE, Yutaka NAKANO, Hiroyuki NAKAMOTO, "A precise classifier for the substances in urinary sediment images based on neural networks and fuzzy reasoning", *Institute of Electrical and Electronics Engineers,* Vol. 3, No. 2, 2000, pp. 128 - 133.

[44] Li-Yan Dong, Sen-Miao Yuan, Guang-Yuan Liu and Ling-Yan Zhou, "Classification of Urinary Sediments Image Based on Bayesian Classifier", *Mechatronics and Automation*, Vol.10, No.2, 2007, pp. 556 - 560.

[45] Sabiq Adzhani Hammam1, Tito Waluyo Purboyo, and Randy Erfa Saputra, "A Review Application Of Image Segmentation On Statistical Texture Analysis, *"International Journal of Applied Engineering Research,* Vol. 12, No. 20, 2017, pp. 169-175.

Annex

Adaptive media Filtering

```
%#codegen
function [pixel_val, pixel_valid] = mlhdlc_median_filter(c_data, c_idx)

%   Copyright 2011-2015 The MathWorks, Inc.

smax = 9;
persistent window;
if isempty(window)
   window = zeros(smax, smax);
end

cp = ceil(smax/2); % center pixel;

w3 = -1:1;
w5 = -2:2;
w7 = -3:3;
w9 = -4:4;

r3 = cp + w3;      % 3x3 window
r5 = cp + w5;      % 5x5 window
r7 = cp + w7;      % 7x7 window
r9 = cp + w9;      % 9x9 window

d3x3 = window(r3, r3);
d5x5 = window(r5, r5);
d7x7 = window(r7, r7);
d9x9 = window(r9, r9);

center_pixel = window(cp, cp);


% use 1D filter for 3x3 region
outbuf = get_median_1d(d3x3(:)');
```

```
[min3, med3, max3] = getMinMaxMed_1d(outbuf);

% use 2D filter for 5x5 region
outbuf = get_median_2d(d5x5);
[min5, med5, max5] = getMinMaxMed_2d(outbuf);

% use 2D filter for 7x7 region
outbuf = get_median_2d(d7x7);
[min7, med7, max7] = getMinMaxMed_2d(outbuf);

% use 2D filter for 9x9 region
outbuf = get_median_2d(d9x9);
[min9, med9, max9] = getMinMaxMed_2d(outbuf);


pixel_val = get_new_pixel(min3, med3, max3, ...
   min5, med5, max5, ...
   min7, med7, max7, ...
   min9, med9, max9, ...
   center_pixel);


% we need to wait until 9 cycles for the buffer to fill up
% output is not valid every time we start from col1 for 9 cycles.
persistent datavalid
if isempty(datavalid)
   datavalid = false;
end
pixel_valid = datavalid;
datavalid = (c_idx >= smax);


% build the 9x9 buffer
window(:,2:smax) = window(:,1:smax-1);
window(:,1) = c_data;

end
```

```
%%%%%%%%%%%%%%%%%%%%%%%%%%%%%%%%%%%%%%%%%%%%%%%%%%%%
%%%%%%%%%%%%%%%%%%
function [min, med, max] = getMinMaxMed_1d(inbuf)

max = inbuf(1);
med = inbuf(ceil(numel(inbuf)/2));
min = inbuf(numel(inbuf));

end

%%%%%%%%%%%%%%%%%%%%%%%%%%%%%%%%%%%%%%%%%%%%%%%%%%%%
%%%%%%%%%%%%%%%%%%
function [min, med, max] = getMinMaxMed_2d(inbuf)

[nrows, ncols] = size(inbuf);
max = inbuf(1, 1);
med = inbuf(ceil(nrows/2), ceil(ncols/2));
min = inbuf(nrows, ncols);

end

%%%%%%%%%%%%%%%%%%%%%%%%%%%%%%%%%%%%%%%%%%%%%%%%%%%%
%%%%%%%%%%%%%%%%%%
function new_pixel  = get_new_pixel(...
    min3, med3, max3, ...
    min5, med5, max5, ...
    min7, med7, max7, ...
    min9, med9, max9, ...
    center_data)

if (med3 > min3 && med3 < max3)
    new_pixel = get_center_data(min3, med3, max3,center_data);
elseif (med5 > min5 && med5 < max5)
    new_pixel = get_center_data(min5, med5, max5,center_data);
elseif (med7 > min7 && med7 < max7)
    new_pixel = get_center_data(min7, med7, max7,center_data);
elseif (med9 > min9 && med9 < max9)
```

```
    new_pixel = get_center_data(min9, med9, max9,center_data);
else
    new_pixel = center_data;
end

end

%%%%%%%%%%%%%%%%%%%%%%%%%%%%%%%%%%%%%%%%%%%%%%%%%%%%%%%%%%%%%%%%%%%%%%%%%%%%%%%%%%%%%%%%%%
function [new_data] = get_center_data(min,med,max,center_data)
if center_data <= min || center_data >= max
    new_data = med;
else
    new_data = center_data;
end
end

%%%%%%%%%%%%%%%%%%%%%%%%%%%%%%%%%%%%%%%%%%%%%%%%%%%%%%%%%%%%%%%%%%%%%%%%%%%%%%%%%%%%%%%%%%
% perform median 1d computation
%%%%%%%%%%%%%%%%%%%%%%%%%%%%%%%%%%%%%%%%%%%%%%%%%%%%%%%%%%%%%%%%%%%%%%%%%%%%%%%%%%%%%%%%%%
function outbuf = get_median_1d(inbuf)

numpixels = length(inbuf);

tbuf = inbuf;

for ii=coder.unroll(1:numpixels)
    if bitand(ii,uint32(1)) == 1
        tbuf = compare_stage1(tbuf);
    else
        tbuf = compare_stage2(tbuf);
    end
end

outbuf = tbuf;
```

```
end

function outbuf = compare_stage1(inbuf)
numpixels = length(inbuf);
tbuf = compare_stage(inbuf(1:numpixels-1));
outbuf = [tbuf(:)' inbuf(numpixels)];
end

function outbuf = compare_stage2(inbuf)
numpixels = length(inbuf);
tbuf = compare_stage(inbuf(2:numpixels));
outbuf = [inbuf(1) tbuf(:)'];
end

function [outbuf] = compare_stage(inbuf)

step = 2;
numpixels = length(inbuf);

outbuf = inbuf;

for ii=coder.unroll(1:step:numpixels)
   t = compare_pixels([inbuf(ii), inbuf(ii+1)]);
   outbuf(ii) = t(1);
   outbuf(ii+1) = t(2);
end

end

function outbuf = compare_pixels(inbuf)
if (inbuf(1) > inbuf(2))
   outbuf = [inbuf(1), inbuf(2)];
else
   outbuf = [inbuf(2), inbuf(1)];
end
end
```

```
%%%%%%%%%%%%%%%%%%%%%%%%%%%%%%%%%%%%%%%%%%%%%%%%%%%%%%%%%%%%%%%%%%%%%%%%%%%%%%%%%%%
%%%%%%%%%%%%%%%%%%%%%
% perform median 2d computation
%%%%%%%%%%%%%%%%%%%%%%%%%%%%%%%%%%%%%%%%%%%%%%%%%%%%%%%%%%%%%%%%%%%%%%%%%%%%%%%%%%%
%%%%%%%%%%%%%%%%%%%%%
function outbuf = get_median_2d(inbuf)


outbuf = inbuf;
[nrows, ncols] = size(inbuf);
for ii=coder.unroll(1:ncols)
    colData = outbuf(:, ii)';
    colDataOut = get_median_1d(colData)';
    outbuf(:, ii) = colDataOut;
end
for ii=coder.unroll(1:nrows)
    rowData = outbuf(ii, :);
    rowDataOut = get_median_1d(rowData);
    outbuf(ii, :) = rowDataOut;
end


end
type(testbench_name);
%   Copyright 2011-2015 The MathWorks, Inc.


I = imread('mlhdlc_img_pattern_noisy.tif');
J = I;


smax = 9;
[nrows, ncols] = size(I);
ll = ceil(smax/2);
ul = floor(smax/2);


for ii=1:ncols-smax
    for jj=1:nrows-smax


        c_idx = ii;
```

```
        c_data = double(I(jj:jj+smax-1, ii));

        [pixel_val, pixel_valid] = mlhdlc_median_filter(c_data, c_idx);

        if pixel_valid
            J(jj, ii) = pixel_val;
        end
    end
end


h = figure;
set( h, 'Name', [ mfilename, '_plot' ] );
subplot( 1, 2, 1 );
imshow( I, [  ] );
subplot( 1, 2, 2 );
imshow( J, [  ] );
```

Signed Declaration Sheet

I, the undersigned, declare that this thesis is my original work and has not been presented for a degree in any other university, and that all source of materials used for the thesis have been duly acknowledged.

Declared by:

Name: _____

Signature: _____

Date: _____

Confirmed by Advisor:

Name: _____

Signature: _____

Date: _____